by platelet count, serum hyaluronic acid and ultrasonographical findings; it is known that chronic hepatitis C patients presenting with serum hyaluronic acid < 50 ng/ml correspond to the absence of severe fibrosis (35). Moreover, more than 90% of HCV carriers with PNALT presenting with platelet count more than $150 \times 10^3/\mu l$ are reported to have normal or mild liver histologies (20). Although percutaneous liver biopsies could not be performed in our patients, selection according to the above strict criteria enabled us to confidently exclude the possibility of IR caused by advanced fibrosis. Low APRIs in both groups also confirm the relevance of our selection criteria.

Under these conditions, we were able to discover that serum γ-GT was closely associated with HOMA-IR in non-obese, non-diabetic, non-alcoholic and non-steatotic HCV carriers with PNALT. These results are consistent with those of previous studies in that serum γ-GT is an important risk indicator for developing metabolic syndrome and type-2 diabetes (36, 37). A positive association between serum γ-GT and hepatic TNF-α expression has been documented in patients with chronic HCV infection (38). Because an activated TNF-α system is one of the major causes of IR development (15), the close relationship seen between serum γ-GT and HOMA-IR may partially reflect the local enhancement of TNF-α expression in HCV-infected livers. Although serum γ-GT is a non-specific marker of liver injury, it may also become a useful predictor of IR in HCV-infected patients.

Interestingly, serum HCV core protein concentration was not associated with HOMA-IR, which was inconsistent with a previous report demonstrating an association between HOMA-IR and the amount of serum HCV core antigen (14). Although the direct contribution of core protein to the pathogenesis of HCV-induced IR has been shown in transgenic mouse lines (14, 15), recent studies have uncovered that the occurrence of core protein-induced IR is not derived from the protein's intrinsic effect. For example, in mice constitutively expressing HCV core protein, deletion of the proteasome activator PA28γ gene did not induce hyperinsulinaemia or IR, despite the presence of core protein (39). Moreover, we obtained similar results from peroxisome proliferator-activated receptor α-null mice bearing the core protein gene (40). Thus, the results in this study support the notion that the core protein itself does not have the potential to induce IR.

In humans, the relationship between serum adiponectin and presence of HCV is a matter of controversy. Several studies have reported that low adiponectin is significantly associated with high HOMA-IR in patients with chronic hepatitis C (41, 42). On the other hand, a recent large-scale study has clearly shown that chronic HCV infection has little influence on serum adiponectin (43). Here, we also demonstrated no correlation between HOMA-IR and serum adiponectin in non-steatotic HCV-infected patients with PNALT, as well as no differences in adiponectin levels compared with matched HBV carriers. Our results lead us to conclude that the probability of HCV itself modulating adiponectin expression is low.

Also, in this study, serum hsCRP, a surrogate marker of subclinical systemic inflammation, did not differ between HCV and HBV carriers. It has been documented by a case–control study that serum levels of pro-inflammatory cytokines inducing IR, such as TNF-α and interleukin-6, were higher in patients with chronic hepatitis C than in those with other causes of hepatitis, despite similar levels of hepatitis activity (19). Thus, activation of TNF-α-mediated pathway may contribute to HCV-specific IR.

The present study suggests the contribution of the hepatic inflammatory component to the development of IR in chronic hepatitis C. However, our results do not necessarily mean that IR frequently found in chronic hepatitis C patients is mediated by hepatitis alone. HOMA-IR was reported to be higher in patients with chronic hepatitis C than in those with other causes of hepatitis, independent of severity of hepatic inflammation and fibrosis (2, 19), indicating the diabetogenic potential of HCV. HCV might lead to a latent disturbance of the insulin signalling cascade, which cannot be detected by a simple indicator (i.e. HOMA-IR), and trigger IR in cooperation with other factors such as hepatitis.

Clinically, it is well known that elevated HOMA-IR is one of the primary predictors of hyporesponsiveness or failure of interferon therapy in persistently HCV-infected patients (44, 45). The demonstration of a strong relationship between HOMA-IR and waist circumference, serum γ-GT and TG in HCV-infected humans without obesity, diabetes, hepatocyte damage, hepatitis or obvious steatosis indicates that simple nutritional intervention and exercise to reduce visceral fat mass can further ameliorate the outcome of antiviral therapy. In addition, the combination therapy of insulin-sensitizing TG-lowering agents and interferon injections might prove beneficial. In fact, additional treatment with bezafibrate, a typical TG-lowering agent (46), was reported to achieve a higher complete response rate with interferon and ribavirin combination therapy (47). Therefore, accurate evaluation of metabolic disturbances, such as visceral fat accumulation and high levels of serum TG and HOMA-IR, and the ensuing steps taken to regulate

them, round out a list of therapeutic strategies for HCV-infected patients.

There are some limitations in the present study. Firstly, the sample size is limited. Large-scale case–control studies using the same selection criteria will be able to further ascertain the association between HCV infection and development of IR. Secondly, the patients were selected from a homogenous race (i.e. Japanese), and the pathogenesis of HCV-specific IR might differ between races. Finally, we were not able to access the changes in IR with ageing, necessitating further long-term follow-up of our patients to address the issue.

In conclusion, the results of this study demonstrate that the presence of HCV *per se* cannot induce IR; rather, it may be other factors, such as the presence of active hepatitis, hepatic steatosis or fibrosis, that are important to HCV-specific IR. In addition, waist circumference and serum γ-GT and TG were strongly associated with HOMA-IR in non-obese, non-alcoholic and non-steatotic HCV carriers with PNALT, suggesting the likelihood that these parameters are useful and reliable indicators of IR in HCV-infected patients. Although our data offer novel information about the pathogenesis of HCV-specific IR, further large-scale studies are needed to confirm our results.

Acknowledgements

The authors would like to thank nursing and laboratory staff for their skilled work, and Mr Trevor Ralph for his editorial assistance.

Conflicts of interests: none.

References

1. Allison ME, Wreghitt T, Palmer CR, *et al.* Evidence for a link between hepatitis C virus infection and diabetes mellitus in a cirrhotic population. *J Hepatol* 1994; **21**: 1135–9.
2. Mason AL, Lau JY, Hoang N, *et al.* Association of diabetes mellitus and chronic hepatitis C virus infection. *Hepatology* 1999; **29**: 328–33.
3. Mehta SH, Brancati FL, Sulkowski MS, *et al.* Prevalence of type 2 diabetes mellitus among persons with hepatitis C virus infection in the United States. *Ann Intern Med* 2000; **133**: 592–9.
4. Negro F. Insulin resistance and HCV: will new knowledge modify clinical management? *J Hepatol* 2006; **45**: 514–9.
5. Tanaka N, Tanaka E, Sheena Y, *et al.* Useful parameters for distinguishing nonalcoholic steatohepatitis with mild steatosis from cryptogenic chronic hepatitis in the Japanese population. *Liver Int* 2006; **26**: 956–63.
6. Narita R, Abe S, Tabaru A, *et al.* Impact of steatosis on insulin secretion in chronic hepatitis C patients. *Am J Gastroenterol* 2007; **102**: 2173–80.
7. Furutani M, Nakashima T, Sumida Y, *et al.* Insulin resistance/β-cell function and serum ferritin level in non-diabetic patients with hepatitis C virus infection. *Liver Int* 2003; **23**: 294–9.
8. Sumida Y, Kanemasa K, Fukumoto K, *et al.* Hepatic iron accumulation may be associated with insulin resistance in patients with chronic hepatitis C. *Hepatol Res* 2007; **37**: 932–40.
9. Tanaka N, Kiyosawa K. Phlebotomy: a promising treatment for chronic hepatitis C. *J Gastroenterol* 2004; **39**: 601–3.
10. Taura N, Ichikawa T, Hamasaki K, *et al.* Association between liver fibrosis and insulin sensitivity in chronic hepatitis C patients. *Am J Gastroenterol* 2006; **101**: 2752–9.
11. Kruszynska YT, Home PD, McIntyre N. Relationship between insulin sensitivity, insulin secretion and glucose tolerance in cirrhosis. *Hepatology* 1991; **14**: 103–11.
12. Marchesini G, Pacini G, Bianchi G, *et al.* Glucose disposal, beta-cell secretion, and hepatic insulin extraction in cirrhosis: a minimal model assessment. *Gastroenterology* 1990; **99**: 1715–22.
13. Hui JM, Sud A, Farrell GC, *et al.* Insulin resistance is associated with chronic hepatitis C virus infection and fibrosis progression [corrected]. *Gastroenterology* 2003; **125**: 1695–704.
14. Kawaguchi T, Yoshida T, Harada M, *et al.* Hepatitis C virus down-regulates insulin receptor substrates 1 and 2 through up-regulation of suppressor of cytokine signaling 3. *Am J Pathol* 2004; **165**: 1499–508.
15. Shintani Y, Fujie H, Miyoshi H, *et al.* Hepatitis C virus infection and diabetes: direct involvement of the virus in the development of insulin resistance. *Gastroenterology* 2004; **126**: 840–8.
16. Kawaguchi T, Ide T, Taniguchi E, *et al.* Clearance of HCV improves insulin resistance, beta-cell function, and hepatic expression of insulin receptor substrate 1 and 2. *Am J Gastroenterol* 2007; **102**: 570–6.
17. Shoelson SE, Herrero L, Naaz A. Obesity, inflammation, and insulin resistance. *Gastroenterology* 2007; **132**: 2169–80.
18. Parekh S, Anania FA. Abnormal lipid and glucose metabolism in obesity: implications for nonalcoholic fatty liver disease. *Gastroenterology* 2007; **132**: 2191–207.
19. Lecube A, Hernandez C, Genesca J, *et al.* Proinflammatory cytokines, insulin resistance, and insulin secretion in chronic hepatitis C patients: a case–control study. *Diabetes Care* 2006; **29**: 1096–101.
20. Okanoue T, Makiyama A, Nakayama M, *et al.* A follow-up study to determine the value of liver biopsy and need for antiviral therapy for hepatitis C virus carriers with persistently normal serum aminotransferase. *J Hepatol* 2005; **43**: 599–605.
21. Shelmet JJ, Reichard GA, Skutches CL, *et al.* Ethanol causes acute inhibition of carbohydrate, fat, and protein oxidation and insulin resistance. *J Clin Invest* 1998; **81**: 1137–45.

22. Tanaka N, Ichijo T, Okiyama W, *et al.* Laparoscopic findings in patients with nonalcoholic steatohepatitis. *Liver Int* 2006; **26**: 32–8.
23. Arai H, Yamamoto A, Matsuzawa Y, *et al.* Prevalence of metabolic syndrome in the general Japanese population in 2000. *J Atheroscler Thromb* 2006; **13**: 202–8.
24. Ohnishi H, Saitoh S, Takagi J, *et al.* Incidence of insulin resistance in obese subjects in a rural Japanese population: the Tanno and Sobetsu study. *Diabetes Obes Metab* 2005; **7**: 83–7.
25. Wai CT, Greenson JK, Fontana RJ, *et al.* A simple noninvasive index can predict both significant fibrosis and cirrhosis in patients with chronic hepatitis C. *Hepatology* 2003; **38**: 518–26.
26. Liu CH, Lin JW, Tsai FC, *et al.* Noninvasive tests for the prediction of significant hepatic fibrosis in hepatitis C virus carriers with persistently normal alanine aminotransferases. *Liver Int* 2006; **26**: 1087–94.
27. Tanaka N, Sano K, Horiuchi A, Tanaka E, Kiyosawa K, Aoyama T. Highly-purified eicosapentaenoic acid treatment improves nonalcoholic steatohepatitis. *J Clin Gastroenterol* 2008, in press.
28. Tanaka N, Horiuchi A, Yamaura T, *et al.* Efficacy and safety of 6-month iron reduction therapy in patients with hepatitis C virus-related cirrhosis: a pilot study. *J Gastroenterol* 2007; **42**: 49–55.
29. Moriya K, Shintani Y, Fujie H, *et al.* Serum lipid profile of patients with genotype 1b hepatitis C viral infection in Japan. *Hepatol Res* 2003; **25**: 371–6.
30. Sumida Y, Nakashima T, Yoh T, *et al.* Serum thioredoxin elucidates the significance of serum ferritin as a marker of oxidative stress in chronic liver diseases. *Liver* 2001; **21**: 295–9.
31. Petersen KF, Dufour S, Feng J, *et al.* Increased prevalence of insulin resistance and nonalcoholic fatty liver disease in Asian–Indian men. *Proc Natl Acad Sci USA* 2006; **103**: 18273–7.
32. Examination Committee of Criteria for ' Obesity Disease ' in Japan; Japan Society for the Study of Obesity . New criteria for 'obesity disease' in Japan. *Circ J* 2002; **66**: 987–92.
33. Matsuzawa Y, Shimomura I, Nakamura T, *et al.* Pathophysiology and pathogenesis of visceral fat obesity. *Obes Res* 1995; **3**: 187S–94S.
34. Yamashita S, Nakamura T, Shimomura I, *et al.* Insulin resistance and body fat distribution. *Diabetes Care* 1996; **19**: 287–91.
35. Halfon P, Bourliere M, Penaranda G, *et al.* Accuracy of hyaluronic acid level for predicting liver fibrosis stages in patients with hepatitis C virus. *Comp Hepatol* 2005; **4**: 6.
36. Nakanishi N, Suzuki K, Tatara K. Serum γ-glutamyltransferase and risk of metabolic syndrome and type 2 diabetes in middle-aged Japanese men. *Diabetes Care* 2004; **27**: 1427–32.
37. Perry IJ, Wannamethee SG, Shaper AG. Prospective study of serum γ-glutamyltransferase and risk of NIDDM. *Diabetes Care* 1998; **21**: 732–7.
38. Taliani G, Badolato MC, Nigro G, *et al.* Serum concentration of γ-GT is a surrogate marker of hepatic TNF-α mRNA expression in chronic hepatitis C. *Clin Immunol* 2002; **105**: 279–85.
39. Miyamoto H, Moriishi K, Moriya K, *et al.* Involvement of the PA28γ-dependent pathway in insulin resistance induced by hepatitis C virus core protein. *J Virol* 2007; **81**: 1727–35.
40. Tanaka N, Moriya K, Kiyosawa K, *et al.* PPARα activation is essential for HCV core protein-induced hepatic steatosis and hepatocellular carcinoma in mice. *J Clin Invest* 2008; **118**: 683–94.
41. Liu CJ, Chen PJ, Jeng YM, *et al.* Serum adiponectin correlates with viral characteristics but not histologic features in patients with chronic hepatitis C. *J Hepatol* 2005; **43**: 235–42.
42. Jonsson JR, Moschen AR, Hickman IJ, *et al.* Adiponectin and its receptors in patients with chronic hepatitis C. *J Hepatol* 2005; **43**: 929–36.
43. Cua IH, Hui JM, Bandara P, *et al.* Insulin resistance and liver injury in hepatitis C is not associated with virus-specific changes in adipocytokines. *Hepatology* 2007; **46**: 66–73.
44. Romero-Gomez M, Del Mar Viloria M, Andrade RJ, *et al.* Insulin resistance impairs sustained response rate to peginterferon plus ribavirin in chronic hepatitis C patients. *Gastroenterology* 2005; **128**: 636–41.
45. Lecube A, Hernandez C, Simo R, *et al.* Glucose abnormalities are an independent risk factor for nonresponse to antiviral treatment in chronic hepatitis C. *Am J Gastroenterol* 2007; **102**: 2189–95.
46. Aoyama T, Peters JM, Iritani N, *et al.* Altered constitutive expression of fatty acid-metabolizing enzymes in mice lacking the peroxisome proliferator-activated receptor α (PPARα). *J Biol Chem* 1998; **273**: 5678–84.
47. Fujita N, Kaito M, Kai M, *et al.* Effects of bezafibrate in patients with chronic hepatitis C virus infection: combination with interferon and ribavirin. *J Viral Hepat* 2006; **13**: 441–8.

Susceptibility of Chimeric Mice with Livers Repopulated by Serially Subcultured Human Hepatocytes to Hepatitis B Virus

Rie Utoh,[1] Chise Tateno,[1,2] Chihiro Yamasaki,[1] Nobuhiko Hiraga,[3] Miho Kataoka,[1] Takashi Shimada,[4] Kazuaki Chayama,[2,3] and Katsutoshi Yoshizato[1,2,5]

We previously identified a small population of replicative hepatocytes in long-term cultures of human adult parenchymal hepatocytes (PHs) at a frequency of 0.01%-0.09%. These hepatocytes were able to grow continuously through serial subcultures as colony-forming parenchymal hepatocytes (CFPHs). In the present study, we generated gene expression profiles for cultured CFPHs and found that they expressed cytokeratin 19, CD90 (Thy-1), and CD44, but not mature hepatocyte markers such as tryptophan-2,3-dioxygenase (TO) and glucose-6-phosphatase (G6P), confirming that these cells are hepatic progenitor-like cells. The cultured CFPHs were resistant to infection with human hepatitis B virus (HBV). To examine the growth and differentiation capacity of the cells *in vivo*, serially subcultured CFPHs were transplanted into the progeny of a cross between albumin promoter/enhancer-driven urokinase plasminogen activator-transgenic mice and severe combined immunodeficient (SCID) mice. The cells were engrafted into the liver and were able to grow for at least 10 weeks, ultimately reaching a maximum occupancy rate of 27%. The CFPHs in the host liver expressed differentiation markers such as TO, G6P, and cytochrome P450 subtypes and could be infected with HBV. CFPH-chimeric mice with a relatively high replacement rate exhibited viremia and had high serum levels of hepatitis B surface antigen. *Conclusion:* Serially subcultured human hepatic progenitor-like cells from postnatal livers successfully repopulated injured livers and exhibited several phenotypes of mature hepatocytes, including susceptibility to HBV. *In vitro*–expanded CFPHs can be used to characterize the differentiation state of human hepatic progenitor-like cells. (HEPATOLOGY 2008;47:435-446.)

Abbreviations: 9MM, 9-month-old Caucasian male; 10YF, 10-year-old Caucasian female; 12YM, 12-year-old Asian male; 16YF, 16-year-old Asian female; AAT, α1-antitrypsin; AFP, α-fetoprotein; ALB, albumin; BGP, biliary glycoprotein; BrdU, 5-bromo-2′-deoxyuridine; CFPH, colony-forming parenchymal hepatocyte; CK, cytokeratin; G6P, glucose-6-phosphatase; h, human; HBsAg, hepatitis B surface antigen; HBV, hepatitis B virus; CYP, cytochrome P-450; m, mouse; MDR, multidrug resistance protein; MRP, multidrug resistance-associated protein; PH, parenchymal hepatocyte; RI, replacement index; RT-PCR, reverse-transcription polymerase chain reaction; SH, small hepatocyte; TO, tryptophan-2,3-dioxygenase; uPA, urokinase plasminogen activator.

From the [1]Yoshizato Project, Cooperative Link of Unique Science and Technology for Economy Revitalization (CLUSTER), Hiroshima Prefectural Institute of Industrial Science and Technology, Hiroshima, Japan; the [2]Hiroshima University Liver Project Research Center, Hiroshima, Japan; the [3]Division of Frontier Medical Science, Department of Medicine and Molecular Science, Programs for Biomedical Research, Graduate School of Biomedical Sciences, Hiroshima University, Hiroshima, Japan; [4]PhoenixBio Co., Ltd., Hiroshima, Japan; and the [5]Developmental Biology Laboratory and Hiroshima University 21st Century COE Program for Advanced Radiation Casualty Medicine, Department of Biological Science, Graduate School of Science, Hiroshima University, Hiroshima, Japan.

Received March 20, 2007; accepted September 18, 2007.

Supported by the Cooperative Link of Unique Science and Technology for Economy Revitalization (CLUSTER): Promotion of Science and Technology in Regional Areas: Ministry of Education, Culture, Sports, Science and Technology, Japan.

Present address for Rie Utoh: Institute of Advanced Biomedical Engineering and Science, Tokyo Women's Medical University, Tokyo, Japan.

Present address for Chise Tateno, Chihiro Yamasaki, and Katsutoshi Yoshizato: PhoenixBio Co., Ltd., Hiroshima, Japan.

Address reprint requests to: Katsutoshi Yoshizato, Ph.D., PhoenixBio Co., Ltd., 3-4-1 Kagamiyama, Higashihiroshima, Hiroshima 739-0046, Japan. E-mail: katsutoshi.yoshizato@phoenixbio.co.jp; fax: (81)-82-431-0017.

Published online in Wiley InterScience (www.interscience.wiley.com).

DOI 10.1002/hep.22057

Potential conflict of interest: Nothing to report.

Studies using rodents with damaged livers have shown that parenchymal hepatocytes (PHs) have great growth potential. When mouse (*m*) hepatocytes were transplanted into the livers of albumin promoter/enhancer-driven urokinase plasminogen activator (uPA)-transgenic mice,[1] they engrafted and repopulated the host liver. Serial transplantation experiments using *m*-hepatocytes in mice with tyrosinemia showed their enormous growth capacity.[2] The replicative potential of rat hepatocytes has also been demonstrated by transplanting them into the partially hepatectomized liver of a retrorsine-treated rat,[3] and uPA-transgenic mice crossed with severely immunodeficient mice, such as severe combined immunodeficient (SCID)/beige mice,[4] SCID mice,[5,6] or recombination activation gene 2 knockout mice[7] have been used to show the growth potential of human (*h*)-hepatocytes. When transplanted into uPA/SCID mice, PHs from a human juvenile male grew in the host liver to a level at which the proportion (replacement index) of the area of repopulated *h*-hepatocytes to the total number (host and donor) of hepatocytes reached 96% at 64 days posttransplantation.[5] Such *h*-hepatocyte–chimeric mice have been used to study the pharmacological responses of *h*-hepatocytes[5] and to investigate *h*-hepatitis viral infections.[4,6-8]

In contrast, normal hepatocytes have limited replicative capacity *in vitro* and acquire an abnormal phenotype if they are cultured for extended periods.[9,10] Studies on hepatocytes cultured in a newly devised medium (hepatocyte clonal growth medium[11,12]) revealed a subpopulation of highly replicative PHs, known as small hepatocytes (SHs), in both rats[12] and humans.[13] Their occupancy rate in *h*-liver ranged from 0.01% to 0.09% and was dependent on donor age.[13] The *h*-SHs formed colonies and grew continuously through several subcultures, which led us to name them colony-forming PHs (CFPHs).[13] Replication of the CFPHs was donor age–dependent up to passage 7 ($p = 7$),[13] and the cells did not exhibit a normal hepatocytic phenotype. Instead, they exhibited the traits of hepatocytes or biliary cells depending on the culture conditions. In addition, the CFPHs were not susceptible to infection with hepatitis B virus (HBV) (unpublished data).

In this study, we generated gene expression profiles of CFPHs and transplanted serially subcultured CFPHs into homozygous uPA/SCID mice to examine their growth and differentiation capacity. Our results indicate that the cells were engrafted onto the liver parenchyma and repopulated the tissue, ultimately differentiating into mature hepatocytes. Importantly, the *in vitro*–propagated CFPHs became susceptible to infection with HBV. This study supports our previous suggestion that CFPHs from *h*-postnatal liver are hepatic progenitor-like cells with the potential to assume a normal hepatocytic phenotype.[13]

Materials and Methods

h-*Hepatocytes.* This study was performed with the approval of the Hiroshima Prefectural Institute of Industrial Science and Technology Ethics Board. PHs were isolated as described[13,14] from livers donated by a 12-year-old Asian male (12YM) and a 16-year-old Asian female (16YF) according to the guidelines of the 1975 Declaration of Helsinki. Cryopreserved PHs from a 9-month-old Caucasian male (9MM) and a 10-year-old Caucasian female (10YF) were obtained from In Vitro Technologies (Baltimore, MD) and BD Biosciences (San Jose, CA), respectively.

Culture of CFPHs. Cryopreserved PHs from the 9MM, 12YM, and 16YF were thawed[5] and serially subcultured to obtain *in vitro*–expanded CFPHs.[13] Commercial 9MM PHs and freshly isolated 12YM and 16YF PHs were each subcultured to $p = 3$. The expanded cells were then cryopreserved, thawed upon use, and cultured on collagen-coated plates for 14-20 days as described.[13]

Flow Cytometry. We detached 12YM CFPHs ($p = 4$ or 5) from culture plates by treatment with 0.25% Trypsin-EDTA (Invitrogen, Carlsbad, CA), suspended, incubated on ice for 30 minutes with *m*-monoclonal antibodies against *h*Thy-1 (clone F15-42-1; Chemicon, Temecula, CA), and incubated with antibodies against *m*-immunoglobulin G Alexa-488 (Molecular Probes, Eugene, OR). We used *m*-immunoglobulin G_1 as a negative control. The cells were then analyzed and separated using a fluorescence-activated cell sorter (Becton Dickinson, Franklin Lakes, NJ) as reported.[12]

Transplantation of PHs and CFPHs. We detached 9MM and 12YM CFPHs ($p = 4$) from their culture plates and treated for 1 hour with DMEM containing 10% fetal bovine serum and 3 μg/mL anti–*h*-integrin α1 monoclonal antibodies (clone FB12, Chemicon).[15] This procedure improved engraftment of the CFPHs in uPA/SCID *m*-liver and reduced host mortality.

Transplantation of PHs and CFPHs was performed as described previously.[5] Homozygous uPA/SCID mice were injected with 0.75×10^6 9MM and 12YM PHs or $0.75\text{-}1.0 \times 10^6$ *in vitro*–expanded 9MM and 12YM CFPHs into the inferior splenic pole. When necessary, 10 mM 5-bromo-2′-deoxyuridine (BrdU) (Sigma, St. Louis, MO) and 1.2 mM 5-fluoro-2′-deoxyuridine (Wako, Osaka, Japan) in saline were injected intraperitoneally into the mice at 10 μL/g body weight 1 hour prior to death. The animals were treated according to the guidelines of our local committee on animal experiments.

Table 1. Summary of CFPH and PH Transplantation Experiments in uPA/SCID Mice

Group	Donor Cells	Time of Sacrifice (Weeks After Transplantation)	No. of Transplanted Mice	No. of Mice with Engraftment* [RE (%)]	RI† [Mean ± SD (n)]
A	12YM CFPHs (p = 4)	3	9	3 (33)	0.06-0.19% [0.14 ± 0.07% (n = 3)]
B	9MM CFPHs (p = 4)	3	6	4 (67)	0.03-0.05% [0.04 ± 0.01% (n = 4)]
C	9MM PHs	3	3	3 (100)	5.1-19.4% [6.4 ± 2.9% (n = 3)]
D	12YM CFPHs (p = 4)	9-10	27	14 (52)	0.2-27.0% [6.6 ± 8.3% (n = 14)]
E	9MM PHs	10-11	23‡	23 (100)‡	32.6-82.2% [57.4% (n = 2)]
F	12YM PHs	10	6	4 (67)	31.0-77.0% [62.3 ± 23.8% (n = 4)]
G§	12YM CFPHs (p = 4)	17-20	4	ND	ND

Abbreviation: ND, not determined.

*Number of mice whose livers were engrafted with transplanted PHs or CFPHs. The RE was determined via *h*ALB immunohistochemistry on sections prepared from 5 lobes of a liver.

†Ranges of RI of chimeric mice used in each group.

‡Data from Tateno et al.[5]

§Mice from group G were used for HBV infection studies.

We transplanted 9MM and 12YM CFPHs into 6 and 40 uPA/SCID mice, respectively. The mice were then killed 3, 9, or 10 weeks later, depending on the experimental purpose. In a previous report, we used 9MM and 12YM PHs as donor cells.[5] In this study, we used some of the preserved livers from these mice for histological examinations and as sources of RNA for reverse-transcription polymerase chain reaction (RT-PCR) analysis. The mice used in our transplantation experiments were separated into 7 groups (A-G) as shown in Table 1, which includes the rates of engraftment and replacement indices (RIs) of the chimeric mice.

Blood samples (5 μL) were collected periodically after transplantation from the tail veins of the hosts, and the level of *h*-albumin (ALB) in each was determined using a Human Albumin ELISA Quantitation Kit (Bethyl Laboratories, Montgomery, TX) to monitor the growth of the transplanted CFPHs.

RT-PCR. An RNeasy Tissue Kit (Qiagen, Valencia, CA) was used to isolate total RNA from freeze-thawed 9MM and 10YF PHs, cells of the *h*-hepatoma cell line HepG2, and 12YM and 16YF CFPHs (p = 4). RNA was also isolated with Isogen (Nippon Gene, Tokyo, Japan) from the livers of homozygous uPA/SCID mice and mice chimeric for 12YM PHs or 12YM CFPHs. Each RNA sample was treated with deoxyribonuclease (Takara Bio, Kyoto, Japan) and used as the template for RT-PCR. The RNA (1 μg) was reverse-transcribed with random hexamers using PowerScript Reverse Transcriptase (Clontech, Kyoto, Japan). All reactions were performed with Ex Taq (Takara Bio). Semiquantitative PCR was performed to allow linear amplification of the targets. The following *h*-specific or *m* and *h* cross-reactive genes were subjected to RT-PCR under the conditions shown in Supplementary Table 1: ALB, α1-antitrypsin (AAT), tryptophan-2,3-dioxygenase (TO), glucose-6-phosphatase (G6P), α-fetoprotein (AFP), cytokeratin 19 (CK19), biliary glycoprotein (BGP), Thy-1, CD44, multidrug resistance protein 1 (MDR1), multidrug resistance-associated protein 1 (MRP1), MRP2, and glyceraldehyde-3-phosphate dehydrogenase.

In Situ *Hybridization.* Cryosections (7 μm thick) were fixed with 4% paraformaldehyde, then incubated with 100 ng/mL proteinase K for 10 minutes at 37°C. The sections were then treated at 90°C for 6 minutes and hybridized for 2 hours at 37°C with biotinylated h-DNA probes (Dako, Glostrup, Denmark). The sections were also used to detect whole *h*-genomic DNA using the GenPoint System (Dako) according to the manufacturer's instructions. Finally, they were stained with hematoxylin-eosin.

Immunohistochemistry and Histochemistry. Formalin-fixed livers were embedded in paraffin and sectioned 5 μm thick. The sections were heated in a microwave oven for 5 minutes in Target Retrieval Solution (Dako), then placed at room temperature for 20 minutes. The livers used to generate frozen sections were embedded in OCT compound (Sakura Finechemicals, Tokyo, Japan), frozen in liquid nitrogen, and sectioned 5 μm thick. The cultured cells were fixed in cold ethanol for 10 minutes. The primary antibodies and conditions used for immunohistochemistry are listed in Supplementary Table 2. For bright-field immunohistochemistry, the antibodies were visualized using a Vectastain ABC Kit (Vector Laboratories, Burlingame, CA) using DAB substrates. Fluorescense immunohistochemistry was performed using Alexa 488–conjugated or Alexa 594–conjugated secondary antibodies (Molecular Probes). The nuclei were stained with Hoechst 33258. Glycogens were visualized using a periodic acid-Schiff (PAS) staining kit (Muto Pure Chemicals, Tokyo, Japan). RIs were determined using

*h*ALB-immunostained sections of chimeric *m*-livers as reported previously.[5]

HBV Infection. We obtained *h*-serum containing high-titer HBV DNA (8.1 $\log_{10}$ genome equivalents/mL serum) from an HBV genotype C carrier after obtaining informed consent. The serum was kept at −80°C until use. Four CFPH-chimeric mice were intravenously injected with 100 μL of the HBV-positive serum 9-12 weeks after transplantation.

HBV Marker Analysis. Hepatitis B surface antigen (HBsAg) was measured using an Architect Analyzer (Abbott, Osaka, Japan). Serum DNA was extracted using a SMITEST EX-R&D Nucleic Acid Extraction Kit (Genome Science Laboratories, Fukushima, Japan). Small amounts of HBV DNA (<300 copies/mL) were detected via nested PCR.[8] If HBV DNA was detected during the initial round of PCR, the copy number was determined via real-time PCR as reported.[8]

Results

***Phenotypes of CFPHs* In Vitro.** We seeded 9MM and 12YM PHs on culture dishes and confirmed that the CFPHs from the 2 donors were similar in morphology and replicative capacity. A small number of the CFPHs (0.01%-0.09% of the seeded PHs) began to replicate after 5 days, and the number of replicating cells gradually increased until colonies appeared at 17 days (Fig. 1A); after 21 days, the cells covered the surface of the dish (Fig. 1B). Most of the seeded PHs were not replicative, and they gradually flattened, acquiring a senescent morphology within 20 days of seeding (Fig. 1A). The CFPHs showed an epithelial cell–like morphology with scant cytoplasm (Fig. 1B), and they retained this appearance during subculture (Fig. 1C). The population doubling time (PDT) of the CFPHs gradually increased as the passage number increased. Up to p = 4, the CFPHs from the young donors replicated with a population doubling time of 170-220 hours; subsequently, the population doubling time increased until the cells finally became senescent.[13]

The expression of several marker genes was compared among PHs, HepG2 cells, and CFPHs (Fig. 1D). In our experience, no significant differences exist in the marker gene expression profiles of PHs among different donors, and the same trend applies to subcultured CFPHs.[13] At p = 4, the CFPHs expressed less ALB and AAT messenger RNA compared with the PHs. The PHs expressed TO and G6P, both of which are markers of mature hepatocytes, whereas the CFPHs did not. CK19, a hepatic progenitor/biliary cell marker, was expressed in both the CFPHs and HepG2 cells, but not in the PHs. BGP, a cell–cell adhesion molecule in epithelium, endothelium, and myeloid cells,[16] was expressed in the PHs and HepG2 cells, but only faintly in the CFPHs. The CFPHs, but not the PHs or HepG2 cells, expressed Thy-1, a hematopoietic/hepatic progenitor cell marker. AFP, a hepatic progenitor/carcinoma cell marker, was only detectable in HepG2 cells. CD44, an SH[17] or oval cell marker,[18] was strongly expressed in CFPHs, but only faintly in PHs and HepG2 cells. PHs and CFPHs faintly expressed MDR1. PHs expressed MRP2, but not MRP1. In contrast, CFPHs expressed MRP1, but not MRP2. A change from MRP2 to MRP1 expression during culture has been reported in rat hepatocytes.[19]

Thy-1 and CD44 expression in CFPHs was assessed via immunocytochemistry (Fig. 1E-F). A few CFPHs were positive for Thy-1 (Fig. 1E), whereas the majority was strongly positive for CD44 (Fig. 1F). Fluorescence-activated cell sorting indicated that a minor population of the CFPHs expressed Thy-1 (Fig. 1G-H), with an occupancy rate of 1%-3% (Fig. 1H). The CFPHs expressed CK7, CK8, CK18, and CK19 in the preconfluent state and became CK7- and CK19-negative in condensed regions postconfluence (data not shown), which is in agreement with our previous findings.[13] Other hepatic stem cell markers such as CD34 and c-kit were undetectable in our CFPHs (data not shown).

Repopulation of CFPHs in uPA/SCID Mouse Liver. We transplanted 12YM CFPHs (p = 4) into 27 homozygous uPA/SCID mice. The serum concentration of *h*ALB was monitored posttransplantation as a measure of the RI of CFPHs (Fig. 2A). Approximately half of the hosts had no or only a small increase in the level of *h*ALB throughout the experimental period. The remaining mice showed a continuous increase in the concentration of *h*ALB, which reached >10 μg/mL after 9 to 10 weeks. Animal 27 showed the greatest increase, reaching 0.7 mg/mL after 10 weeks. The RI of each of the 14 mice in which blood *h*ALB concentration was >8 μg/mL after 9 to 10 weeks was determined by dividing the *h*ALB-positive areas by the entire area measured,[5] and the data were plotted against the corresponding blood *h*ALB concentrations (Fig. 2B). RIs between 0.2% and 27.0% were well correlated with blood *h*ALB concentrations in the 9-728 μg/mL range.

Livers of mice engrafted with the CFPHs were subjected to immunohistochemical staining for *h*ALB (Fig. 3A-D,H) and *in situ* hybridization using *h*-genomic DNA probes (Fig. 3I). *h*ALB-positive cells were visible within 3 weeks posttransplantation as single cells or small clusters consisting of up to 25 cells (Fig. 3A-B). Larger clusters containing 20-450 *h*ALB-positive cells appeared after 9 to 10 weeks (Fig. 3C for animal 2 and Fig. 3D for animals 17 and 27). To detect replicating CFPHs, the mice were

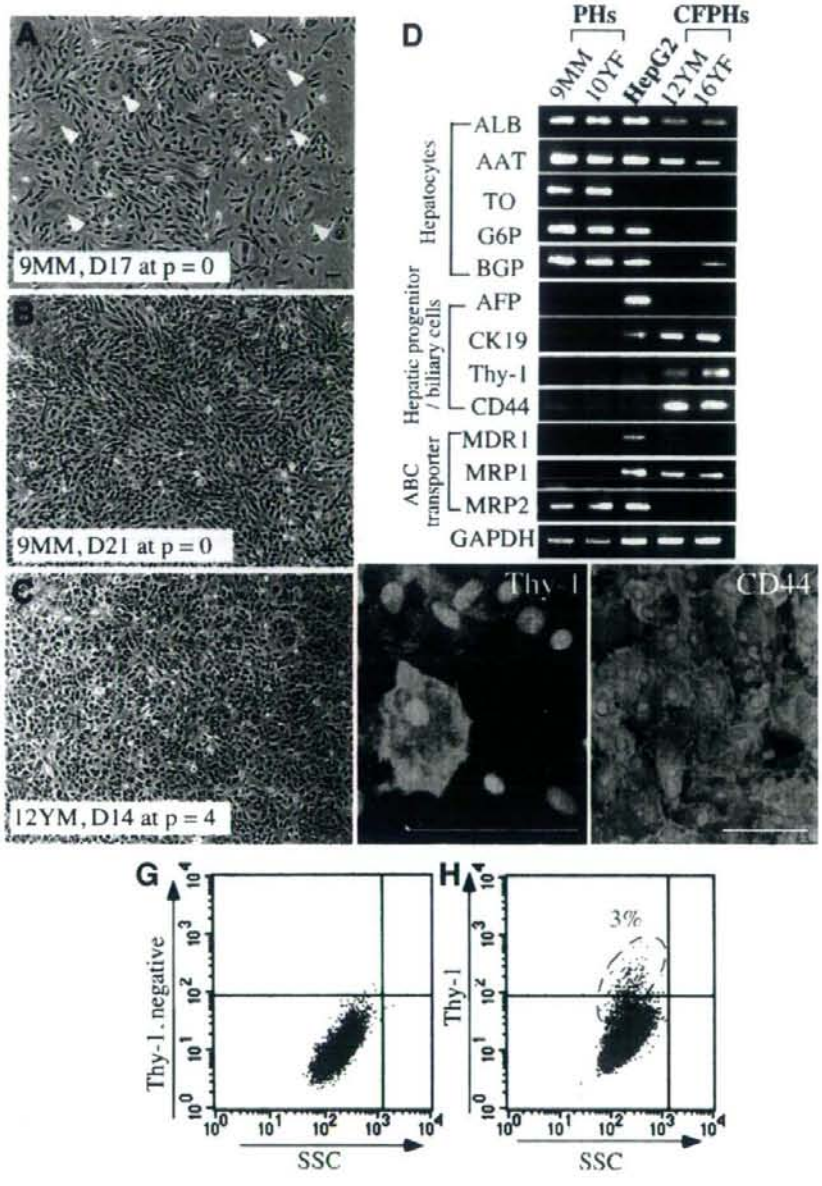

Fig. 1. CFPH growth and gene expression. (A-C) CFPH colony formation. We seeded 9MM PHs at 8×10^3 cells/cm^2 and cocultured with mitomycin C-treated Swiss 3T3 cells in *h*-hepatocyte clonal growth medium. A few CFPHs proliferated and formed colonies. CFPHs were cultured for (A) 17 and (B) 21 days. PHs were nonreplicative and were gradually expelled by replicative CFPHs. Arrowheads indicate the remaining flattened PHs, whose size increased. (C) Cryopreserved 12YM CFPHs (p = 3) were thawed and cultured in *h*-hepatocyte clonal growth medium with Swiss 3T3 cells for 14 days. (D) CFPH messenger RNA expression profiles. RNA was extracted from 9MM and 10YF PHs, HepG2 cells, and 12YM and 16YF CFPHs (p = 4). Semiquantitative RT-PCR was performed for ALB, AAT, TO, G6P, BGP, AFP, CK19, Thy-1, CD44, and the ABC transporters MDR1, MRP1, and MRP2. Glyceraldehyde-3-phosphate dehydrogenase (GAPDH) was used as an internal control. (E,F) Immunohistochemistry of Thy-1 and CD44. 12YM CFPHs (p = 4) were cultured for 14 days and stained for (E) Thy-1 and (F) CD44. The nuclei were stained with Hoechst 33258. Scale bar: 100 μm. (G,H) Flow cytometric analysis of CFPHs for Thy-1. Cells were suspended in Dulbecco's modified Eagle's medium containing 10% fetal bovine serum with (G) *m*-immunoglobulin G_1 as a negative control or (H) anti-*h*Thy-1 antibodies. Living cells were analyzed via fluorescence-activated cell sorting. A small fraction (3% in this case) of the CFPHs was Thy-1 . Three independent analyses were performed with similar results.

given BrdU after 9 weeks. BrdU-positive CFPHs were observed at the edges of the colonies (Fig. 3E-G). Serial liver sections were prepared from CFPH-chimeric mice 9 to 10 weeks after transplantation for *h*ALB immuohistochemistry (Fig. 3H) and for *in situ* hybridization with an *h*-DNA probe (Fig. 3I). The regions identified as containing *h*-hepatocytes by the 2 methods were identical.

Comparison of Repopulation by CFPHs and PHs. PHs and CFPHs (p = 4) were prepared from the livers of 9MM and 12YM donors and transplanted into uPA/SCID mice, and the mice were killed 3 and 10 weeks posttransplantation. The transplanted cells were identified as *h*ALB-positive from histological sections. The number of PH- and CFPH-derived clusters was 125.0 ± 28.2 (n = 3) and 3.3 ± 7.5 (n = 7), respectively, per cross-section of the left lobe of the livers 3 weeks after transplantation, suggesting that the rate of engraftment of the CFPHs was much lower than that of the PHs.

The CFPHs were smaller in size compared with the PHs after 3 weeks (Fig. 4A-B). The cytoplasm of the

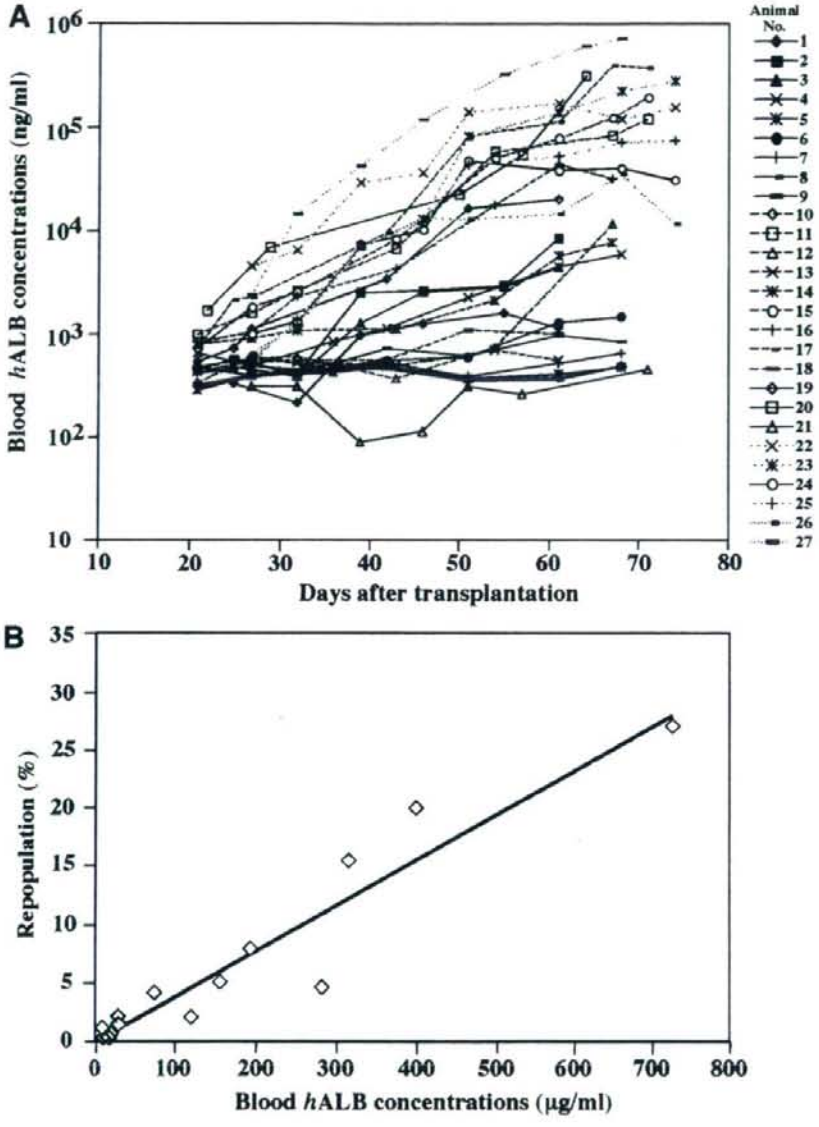

Fig. 2. Transplantation of CFPHs into uPA/SCID mice. The chimeric mice in this experiment are included in group D in Table 1. (A) We transplanted 12YM CFPHs (p = 4) into 27 mice and the serum level of *h*ALB was monitored individually. Ten hosts (animals 1, 5, 6, 7, 8, 9, 10, 13, 18, and 21) did not show significantly elevated *h*ALB levels during the experimental period. Four hosts (2, 3, 4, and 14) showed slight elevation. The *h*ALB concentration of 13 mice (11, 12, 15, 16, 17, 19, 20, 22, 23, 24, 25, 26, and 27) reached >10 μg/mL at 9 to 10 weeks after transplantation. (B) Correlation between the blood *h*ALB level and RI. Fourteen CFPH-chimeric mice (animals 2, 11, 12, 15, 16, 17, 19, 20, 22, 23, 24, 25, 26, and 27) were selected from the mice shown in panel A for RI determination. Their liver sections were immunostained for *h*ALB. RIs were determined for each animal and plotted against the *h*ALB concentration. The correlation coefficient (r^2) between the 2 parameters was 0.91.

former was less abundant and more strongly stained for *h*ALB than that of the latter. We observed *h*CD44 in the plasma membrane of the CFPH-derived cells (Fig. 4E), but not in that of the PH-derived cells (data not shown). At 10 weeks posttransplantation, the CFPHs had increased in size to match those of the PHs, whose sizes were unchanged (Fig. 4C-D), and *h*CD44 expression disappeared from the CFPH-derived cells (Fig. 4F). The diameter of each CFPH and PH was quantified as follows: 18.3 ± 5.1 μm (mean ± SD, n = 65) versus 25.8 ± 6.4 μm (n = 124) at 3 weeks and 27.0 ± 5.5 μm (n = 185) versus 25.8 ± 4.8 μm (n = 187) at 10 weeks. We found no significant differences in this parameter between the 12YM and 9MM samples. Thus, it appears that the CFPHs replicated without changing their original small size until 3 weeks posttransplantation, when they became larger.

Liver sections from the chimeric mice were stained with hematoxylin-eosin to compare the morphological features of PHs and CFPHs at 10 weeks. The repopulated CFPHs (Fig. 4G) showed no significant difference in morphology compared with the repopulated PHs (Fig. 4H). As reported previously,[5,6] the PHs in the chimeric livers were enlarged and had less eosinophilic cytoplasm

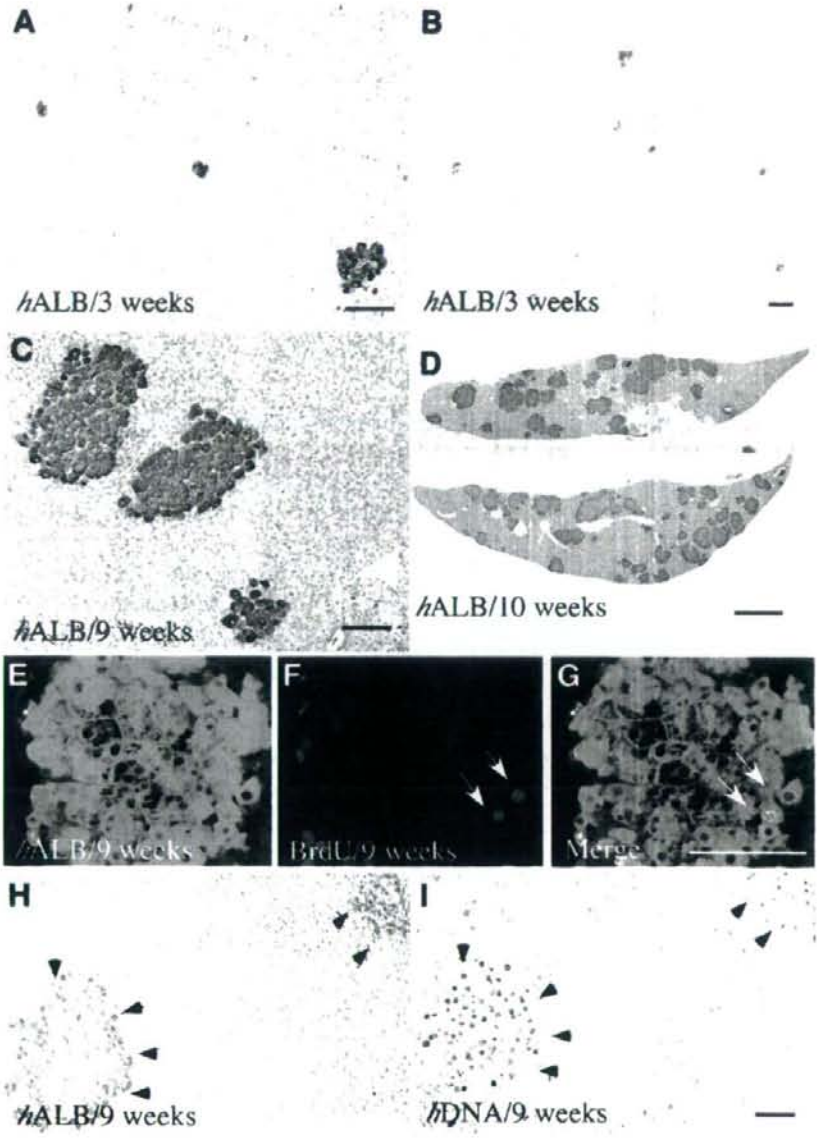

Fig. 3. Engraftment and repopulation of CFPHs in chimeric mouse liver. The chimeric mice in this experiment are included in groups A and D in Table 1. We performed *h*ALB immunohistochemistry using liver sections from CFPH-chimeric mice (A,B) 3, (C) 9, and (D) 10 weeks after transplantation. (A,B) Small clusters composed of 1-25 cells were scattered throughout the liver at 3 weeks in 3 of 9 mice. (C,D) The clusters became larger at 9 to 10 weeks. The liver sections in panel C were prepared from animal 2 in Fig. 2A (RI = 1.1%). The liver sections in panel D were prepared from animals 17 (RI = 20.0%; upper section) and 27 (RI = 27.0%; lower section). Three mice were randomly selected for the BrdU incorporation experiments (animals 2, 19, and 20 in Fig. 2A). They were given BrdU 1 hour before death at 9 weeks posttransplantation. Serial liver sections were subjected to (E) *h*ALB- and (F) BrdU immunohistochemical staining. The image in panel G is panel E and panel F merged. Similar results were obtained from these experiments, and the result from animal 19 (RI = 0.6%) is shown in panels E-G. Serial liver sections were prepared from CFPH-chimeric mice (animals 2, 15, and 17 in Fig. 2A) 9 to 10 weeks after transplantation for *h*ALB immunohistochemistry (H) and for *in situ* hybridization with an *h*-genomic probe (I). Similar results were obtained from the 3 mice. The results shown in panels H and I were obtained from animal 2 (positive cells are indicated by arrowheads). Scale bars in panels A-C, G, and I: 100 μm. Scale bar in panel D: 1 cm.

than the PHs in *h*-livers. The livers of the mice that had low *h*ALB levels at 10 weeks posttransplantation were mostly occupied by red nodules, which have been reported to be formed by the transgene-deleted hepatocytes of the host.[20]

Gene and Protein Expression Profiles of CFPHs in Chimeric Mice Compared with Those of PHs. Three 12YM CFPH-chimeric mice (11, 15, and 17) were randomly selected from the mice in Fig. 2A and killed 10 weeks after transplantation. RNA was extracted from each liver to generate gene expression profiles via RT-PCR. RT-PCR was also performed on 2 12YM PH-chimeric mice that were included in a previous study.[5] The CFPH livers expressed *h*ALB, *h*AAT, *h*TO, *h*G6P, and *h*MRP2, but not *h*CK19, *h*Thy-1, or *h*MRP1, just as in the PH-livers (Fig. 5). Previously, we showed that the PHs in chimeric mice expressed various *h*-cytochrome P450 (*h*CYP) subtypes in a manner similar to the donor liver.[5] In this study, we found that the expression of *h*CYPs 1A2, 2C8, 2C9, 2D6, and 2E1, but not 3A4, in the CFPH-chimeric mice was similar to that in the PH-chimeric mice (data not shown). Expression of *h*CYP3A4 was very

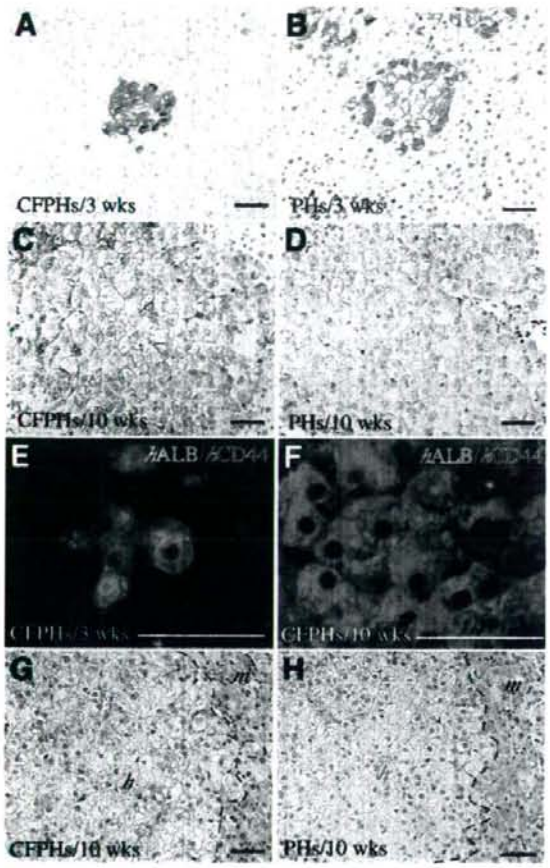

Fig. 4. Immunohistochemical staining for CFPHs and PHs in chimeric mice. Immunohistological analysis with antibodies against (A-D) *h*ALB and (E-F) *h*CD44. We produced 3 12YM CFPH-chimeric mice and 4 9MM CFPH-chimeric mice [(A) and (E), included in groups A and B in Table 1] and 3 9MM PH-chimeric mice [(B), group C], which were killed at 3 weeks posttransplantation. At 10 weeks posttransplantation, 3 12YM CFPH-chimeric mice that were randomly selected from the mice shown in Fig. 2A (15, 16, and 17) were killed [(C) and (F), group D), as were 9MM and 12YM PH-chimeric mice, 2 mice each [(D), groups E and F]. (A-D) Representative images of liver sections prepared from the animals and stained with anti-*h*ALB antibodies. The diameters of the *h*ALB-positive cells were measured in 10-15 randomly selected fields. (E,F) Double-fluorescence immunostaining. Green and red stains depict *h*ALB and *h*CD44, respectively. (G,H) Hematoxylin-eosin staining. (G) Eight CFPH mice were randomly selected from the mice shown in Fig. 2A and killed at 10 weeks posttransplantation. Their liver tissues were then subjected to hematoxylin-eosin staining. (H) Three 12YM PH-chimeric mice were killed at 10 weeks posttransplantation for hematoxylin-eosin staining as above. Similar results were obtained for the 8 CFPH-chimeric mice and 3 PH-chimeric mice. (E-F) Sections from (E) a CFPH-chimeric mouse (RI = 20.0%) and (F) a PH-chimeric mouse (RI = 57%). *h*, *h*-hepatocyte region; *m*, *m*-hepatocyte region. Dashed lines show the boundary between the 2 regions. Scale bars: 50 μm.

low (less than one-fifth) in CFPHs compared with that in PHs.

Protein expression was investigated immunohistochemically for the CFPH-chimeric livers at 3, 9, and 10 weeks posttransplantation. All of the examined CFPHs were Thy-1–negative, CK7-negative, CK19-negative, and AFP-negative (data not shown). The *h*ALB-positive cells were coincident with the *h*CK18-positive cells at both 3 (data not shown) and 9 weeks posttransplantation (Fig. 6A-C). MRP2-positive signals were present on the bile canalicular membranes of the transplanted CFPHs at 10 weeks (Fig. 6D-F). CYP3A4-expressing CFPHs were localized in the pericentral zone (Fig. 6G-I) as reported previously,[21] but their distributions were unique. Although some of the CFPHs were positive for CYP3A4, approximately 70% of them were negative. In contrast, all of the CFPHs in the pericentral zone strongly expressed CYP1A2 (Fig. 6J-L), which is known to be expressed in postnatal liver.[22] The CFPHs in the chimeric mice were strongly PAS-positive (Fig. 6N), whereas the *in vitro* CFPHs were faintly PAS-positive (data not shown). From

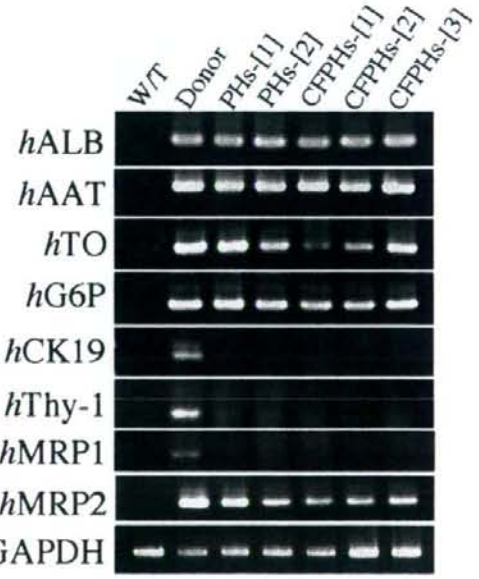

Fig. 5. Gene expression profiles of CFPHs in chimeric mice. Two uPA/SCID mice were transplanted with 12YM PHs ([1] and [2]); 3 uPA/SCID mice were transplanted with 12YM CFPHs ([1], [2], and [3]). The chimeric mice in this experiment are included in groups D and F in Table 1. After 10 weeks, the livers were removed for RT-PCR analysis. At the time of death, the PH-[1]-, PH-[2]-, CFPH-[1]-, CFPH-[2]-, and CFPH-[3]-chimeric mice had RIs of 41.0%, 57.0%, 2.1%, 7.9%, and 20.0%, respectively. The analysis was repeated using liver tissues from donor and uPA/SCID mice without transplantation (W/T). Glyceraldehyde-3-phosphate dehydrogenase (GAPDH) amplification was used as an internal control.

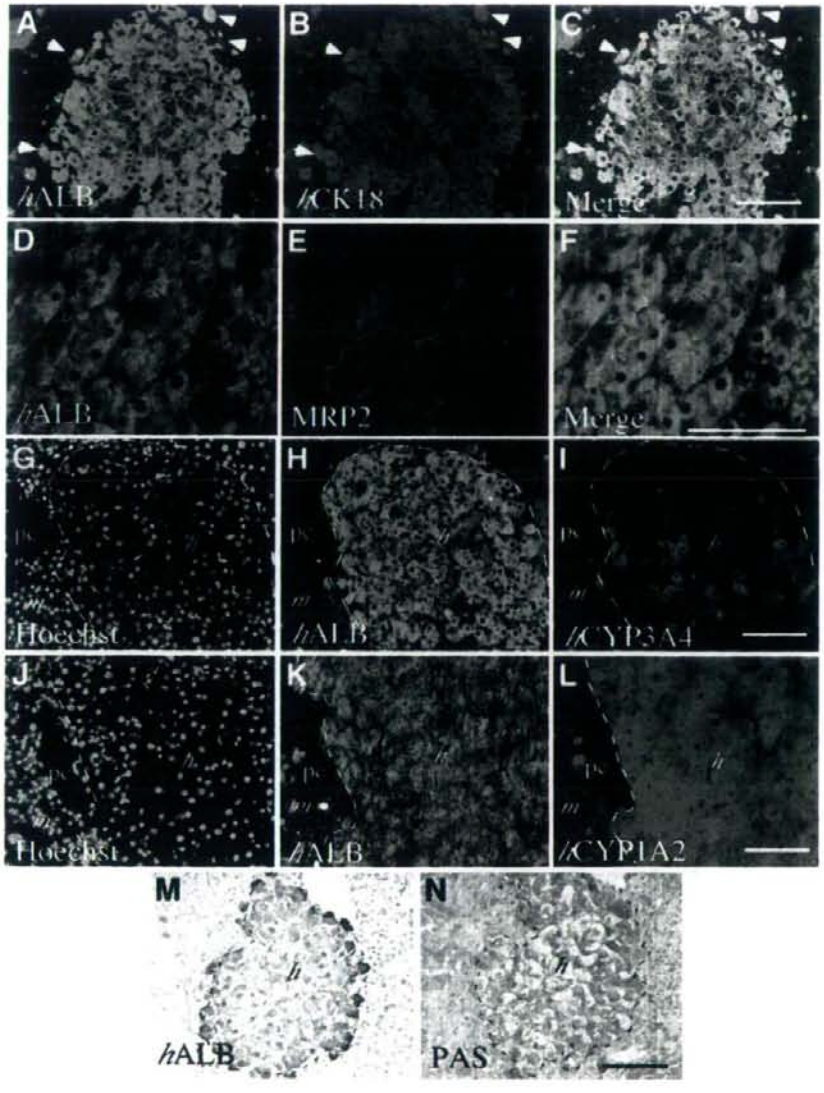

Fig. 6. Protein expression profiles of the CFPHs in chimeric livers. Mice were transplanted with 12YM CFPHs, and their livers were removed 9 to 10 weeks after transplantation for immunohistochemical analysis of (A,D,H,K) *h*ALB, (B) *h*CK18, (E) MRP2, (I) CYP3A4, and (L) CYP1A2. The chimeric mice in this experiment are included in group D in Table 1. Representative images are shown. (A-F) Double-fluorescence immunostaining. (A,D) *h*ALB is stained green. (B) *h*CK18 and (E) *h*MRP2 are stained red. Panels A and B were merged to create panel C; panels D and E were merged to create panel F. The arrowheads in panels A-C show macrophages engulfing such wastes as lipids. Serial sections of liver tissues subjected to 2 series of immunohistochemical examinations, one for (G-I) *h*CYP3A4 and the other for (J-L) *h*CYP1A2. The sections were stained with (G,J) Hoechst 33258, and for (H,K) *h*ALB, (I) *h*CYP3A4, and (L) *h*CYP1A2. Serial sections of liver tissues at 9 weeks posttransplantation were subjected to *h*ALB-immunostaining (M) and PAS staining (N). The positive cells appear brown in (M) and red in (N). *h*, *h*-hepatocyte region; *m*, *m*-hepatocyte region; pc, pericentral zone. Dashed lines show the boundary between the *h*-hepatocyte and *m*-hepatocyte regions. Scale bars: 100 μm.

these results, we conclude that the transplanted CFPHs differentiated into functionally mature hepatocytes. No *h*-cell tumors were formed during any of our experiments in the uPA/SCID mice.

Infection of CFPH-Chimeric Mice with HBV. To further examine whether CFPHs had exhibited normal differentiated phenotypes in chimeric mice, we tested their susceptibility to HBV infection. Four CFPH-chimeric mice with various serum *h*ALB levels (0.2, 1.6, 7.3, and 222.0 μg/mL) were inoculated with 100 μL of HBV-positive *h*-serum at 9-12 weeks posttransplantation. The animals were then tested every 2 weeks for HBV viremia and serum *h*ALB levels (Fig. 7A). The amount of HBV DNA in the animals increased between 2 and 8 weeks after inoculation, and all 4 mice developed measurable viremia within 8 weeks. However, a correlation was observed between the HBV DNA and/or HBsAg level and the *h*ALB level: the former appeared to be high when the latter was high (Fig. 7A). HBsAg was detectable in the serum of the chimeric mice when they showed elevated virus titers: the HBsAg levels of chimeric mice with HBV DNA levels of 2×10^3, 5.2×10^5, 5.9×10^7, and 7.7×10^8 copies/mL 8 weeks after inoculation were <0.05, <0.05, 3.2, and 124.0 IU/mL, respectively. HBV was infectious to CFPH-chimeric mice with very low levels of *h*ALB ($<10^4$ ng/mL), and all mice showed quantitatively

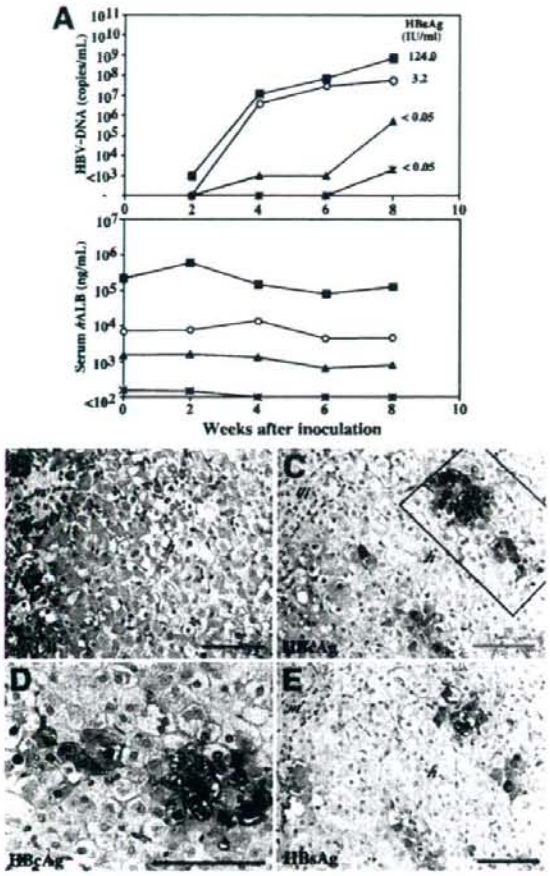

Fig. 7. Susceptibility of chimeric mice to infection with HBV. The chimeric mice in this experiment are included in group G in Table 1. uPA/SCID mice were transplanted with 12YM CFPH (p = 4). (A) The serum *h*ALB concentration of each mouse was determined 9-12 weeks posttransplantation just before the mouse was intravenously injected with 100 μL of HBV-positive *h*-serum (0.2 μg/mL at 12 weeks, 1.6 μg/mL at 10 weeks, 7.3 μg/mL at 11 weeks, and 222.0 μg/mL at 9 weeks). The animals were examined every 2 weeks for HBV viremia and serum *h*ALB level. The upper and lower graphs show the HBV DNA levels (copies/mL) and serum *h*ALB concentrations (ng/mL), respectively. The amount of HBV DNA ($<10^3$ copies/mL) was semiquantitatively measured via nested PCR. The values in the upper graph represent the HBsAg levels at 8 weeks. (B-E) Immunohistochemical analysis of chimeric livers infected with HBV. Serial sections of liver tissues at 8 weeks after inoculation were stained for (B) *h*ALB, (C,D) hepatitis B core antigen, and (E) HBsAg. The region enclosed by a square in panel C is magnified in panel D. Scale bars: 100 μm.

measurable viremia ($>10^3$ copies/mL) up to 8 weeks after inoculation. In contrast, most PH-chimeric mice with $<10^4$ ng/mL *h*ALB did not show quantitatively measurable levels of viremia up to 12 weeks after inoculation (data not shown) as reported previously.[8] In this study, we confirmed that CFPHs were not susceptible to infection with HBV prior to transplantation. The presence of hepatitis B core antigen and HBsAg in the CFPHs from HBV-infected chimeric livers was examined immunohistochemically (Fig. 7C,E). CFPHs were positive for both antigens that were sporadically distributed in the same regions among the CFPH colonies. Hepatitis B core antigen–positive cells accounted for 18.7 ± 8.3% of the total number of CFPHs (n = 3; total cell count = 1,215) (Fig. 7C), and both the nucleus and cytoplasm of the cells showed signals (Fig. 7D).

Discussion

This study supports our previous conclusion that CFPHs are *h*-hepatic progenitor-like cells.[13] Cultured CFPHs expressed such hepatic progenitor cell markers as CK19, Thy-1, and CD44, but not mature hepatocyte markers such as TO and G6P. We also found that *in vitro*–expanded CFPHs in uPA/SCID mice were able to repopulate the parenchyma, in which they differentiated into mature hepatocytes. FISH (fluorescence *in situ* hybridization) using mouse X chromosome probes showed that the engrafted and propagated CFPHs did not fuse to the mouse cells (data not shown). Thus, replicative CFPHs isolated from postnatal liver are normal, functional hepatocyte progenitor-like cells.

The existence of stem/progenitor cells in the adult liver is controversial.[23-25] In the present study, we showed that the CFPHs expressed CK19, Thy-1, and CD44, but not AFP, in serial culture. Thy-1 antigens are expressed in *h*-hepatic progenitor cells in fetal liver[26] and in rat oval cells,[27] but not in normal adult hepatocytes. We showed that Thy-1-expressing cells were present among the CFPHs at an occupancy of 1%-3%. SHs show greater growth potential than PHs in rats.[12] Other studies have reported that CD44 is a specific marker for rat SHs *in vitro* and *in vivo*, and that its expression level decreases with SH maturation *in vitro*.[17] Moreover, a recent study demonstrated that CD44 was strongly expressed by oval cells in a 2-acetylaminofluorene/partial hepatectomy, a D-galactosamine, and a retrorsine/partial hepatectomy rat model, but not by small hepatocyte-like progenitor cells (SHPCs)[18] that appeared in a retrorsine/partial hepatectomy model.[28] We detected CD44 expression in CFPHs at the plasma membrane. These results suggest that Thy-1 and CD44 may be common markers for both rat and *h*-hepatic progenitor cells.

Mouse embryonic liver stem cell lines differentiate into both hepatocytes and bile ducts in uPA/SCID mice.[29] Like PHs, our CFPHs differentiated into mature hepatocytes, but not into biliary epithelial cells, in uPA/SCID mice. CFPHs are considered to be hepatic progenitor-like cells, like rat SHs[12,30-33] and SHPCs.[28,34] SHPCs are

closely related to SHs; they are small and similar in size,[28,30] and both express CYP3A1 and 2E1 at a low level.[28,32] At 3 weeks posttransplantation, the CFPHs were small in size, had a large nucleus-to-cytoplasm ratio, and expressed *h*CD44, but not *h*CK19. At 10 weeks, the cells became bigger, assumed a morphology similar to that of PH-derived cells, and lost their expression of *h*CD44. The expression of *h*CYP3A4 was quite low (0.15-fold) among CFPHs compared with that of PHs (data not shown). In addition, the distribution of *h*CYP3A4-expressing CFPHs in the pericentral zone was unique: more than two-thirds of CFPHs did not express CYP3A4. In the case of the *h*-PH–chimeric mice, all PHs in the pericentral zone expressed CYP3A4 (data not shown).

Presently, we lack experimental data to explain the expression of *h*CYP3A4 in CFPH-chimeric liver, but CFPHs may require some specific environmental factor(s) for differentiation, which might be absent from mouse liver. Alternatively, some factors that specifically inhibit the differentiation of CFPHs might be present there. CK7-positive *h*-hepatic progenitor cells are present in the livers of uPA/SCID mice transplanted with *h*-postnatal liver-derived PHs,[6] and these small cells are strongly immunoreactive to pan-cytokeratin with scant cytoplasm. The CFPHs were morphologically similar to these cells at 3 weeks posttransplantation, although we were unable to detect CK7-positive cells in either the PH- or CFPH-transplanted chimeric livers. However, CFPHs were *h*CK7-, *h*CK19-, and *h*CD44-positive, at least until 1 day posttransplantation (data not shown).

We reported previously that uPA/SCID livers were nearly completely replaced with young donor PHs at 10 weeks posttransplantation.[5] In contrast, the RIs of our CFPH-chimeric mice were <30% at 9 to 10 weeks. CFPHs were rare in the host liver at 3 weeks posttransplantation, whereas several PHs were observed. The lower RIs of the CFPHs might be attributable to their lower engraftment efficiency.

In conclusion, *h*-hepatocytes in immunodeficient, and liver-injured mice are useful for the study of viral hepatitis. Repopulated *h*-hepatocytes are susceptible to infection with HBV[6-8] and HCV.[4,6] Additionally, *h*-hepatocyte–chimeric mice are usually produced by transplanting fresh[6,7] or cryopreserved hepatocytes,[4,5] but sources of *h*-hepatocytes are limited. Several studies have reported on liver repopulation by *in vitro*–propagated cells from adult and fetal livers, such as immortalized mouse hepatic stem cells,[29] rat SHPCs,[34] immortalized *h*-hepatocytes transfected with full-length HBV,[35] and fetal *h*-epithelial/hepatic progenitor cells.[36,37] However, the RIs in these studies were extremely low (less than a few percent). In the present study, we were able to produce CFPH-chimeric mice with RIs as high as 27%. Thus, CFPHs could be an alternative to *h*-hepatocytes as a source of hepatocytes for transplantation. Moreover, the CFPH-chimeric mice were susceptible to infection with HBV, even though their serum *h*ALB levels were extremely low (10^2-10^3 ng/mL). CFPH-chimeric mice will be useful for studying *h*-HBV and for characterizing *h*-hepatic progenitor cells.

Acknowledgment: We thank H. Kohno, Y. Matsumoto, S. Nagai, A. Tachibana, Y. Yoshizane, and Y. Seo for providing technical assistance. We also thank Dr. K. Ohashi (Tokyo Women's Medical University) for helpful discussion and comments during the preparation of this manuscript.

References

1. Rhim JA, Sandgren EP, Degen JL, Palmiter RD, Brinster RL. Replacement of diseased mouse liver by hepatic cell transplantation. Science 1994; 263:1149-1152.
2. Overturf K, Al-Dhalimy M, Ou CN, Finegold M, Grompe M. Serial transplantation reveals the stem-cell-like regenerative potential of adult mouse hepatocytes. Am J Pathol 1997;151:1273-1280.
3. Laconi E, Oren R, Mukhopadhyay DK, Hurston E, Laconi S, Pani P, et al. Long-term, near-total liver replacement by transplantation of isolated hepatocytes in rats treated with retrorsine. Am J Pathol 1998;153:319-329.
4. Mercer DF, Schiller DE, Elliott JF, Douglas DN, Hao C, Rinfret A, et al. Hepatitis C virus replication in mice with chimeric human livers. Nat Med 2001;7:927-933.
5. Tateno C, Yoshizane Y, Saito N, Kataoka M, Utoh R, Yamasaki C, et al. Near completely humanized liver in mice shows human-type metabolic responses to drugs. Am J Pathol 2004;165:901-912.
6. Meuleman P, Libbrecht L, De Vos R, de Hemptinne B, Gevaert K, Vandekerckhove J, et al. Morphological and biochemical characterization of a human liver in a uPA-SCID mouse chimera. HEPATOLOGY 2005;41: 847-856.
7. Dandri M, Burda MR, Török E, Pollok JM, Iwanska A, Sommer G, et al. Repopulation of mouse liver with human hepatocytes and *in vivo* infection with hepatitis B virus. HEPATOLOGY 2001;33:981-988.
8. Tsuge M, Hiraga N, Takaishi H, Noguchi C, Oga H, Imamura M, et al. Infection of human hepatocyte chimeric mouse with genetically engineered hepatitis B virus. HEPATOLOGY 2005;42:1046-1054.
9. Kocarek TA, Schuetz EG, Guzelian PS. Biphasic regulation of cytochrome P450 2B1/2 mRNA expression by dexamethasone in primary cultures of adult rat hepatocytes maintained on matrigel. Biochem Pharmacol 1994; 48:1815-1822.
10. Arterburn LM, Zurlo J, Yager JD, Overton RM, Heifetz AH. A morphological study of differentiated hepatocytes *in vitro*. HEPATOLOGY 1995;22: 175-187.
11. Tateno C, Yoshizato K. Growth and differentiation in culture of clonogenic hepatocytes that express both phenotypes of hepatocytes and biliary epithelial cells. Am J Pathol 1996;149:1593-1605.
12. Tateno C, Takai-Kajihara K, Yamasaki C, Sato H, Yoshizato K. Heterogeneity of growth potential of adult rat hepatocytes *in vitro*. HEPATOLOGY 2000;31:65-74.
13. Yamasaki C, Tateno C, Ararani A, Ohnishi C, Katayama S, Kohashi T, et al. Growth and differentiation of colony-forming human hepatocytes *in vitro*. J Hepatol 2006;44:749-757.
14. Hino H, Tateno C, Sato H, Yamasaki C, Katayama S, Kohashi T, et al. A long-term culture of human hepatocytes which show a high growth poten-

tial and express their differentiated phenotypes. Biochem Biophys Res Commun 1999;256:184-191.
15. Kocken JM, de Heer E, Borel Rinkes IH, Sinaasappel M, Terpstra OT, Bruijn JA. Blocking of $\alpha 1\beta 1$ integrin strongly improves survival of hepatocytes in allogeneic transplantation. Lab Invest 1997;77:19-28.
16. Prall F, Nollau P, Neumaier M, Haubeck HD, Drzeniek Z, Helmchen U, et al. CD66a (BGP), an adhesion molecule of the carcinoembryonic antigen family, is expressed in epithelium, endothelium, and myeloid cells in a wide range of normal human tissues. J Histochem Cytochem 1996;44:35-41.
17. Kon J, Ooe H, Oshima H, Kikkawa Y, Mitaka T. Expression of CD44 in rat hepatic progenitor cells. J Hepatol 2006;45:90-98.
18. Yovchev MI, Grozdanov PN, Joseph B, Gupta S, Dabeva MD. Novel hepatic progenitor cell surface markers in the adult rat liver. HEPATOLOGY 2007;45:139-149.
19. Rippin SJ, Hagenbuch B, Meier PJ, Stieger B. Cholestatic expression pattern of sinusoidal and canalicular organic anion transport systems in primary cultured rat hepatocytes. HEPATOLOGY 2001;33:776-782.
20. Sandgren EP, Palmiter RD, Heckel JL, Daugherty CC, Brinster RL, Degen JL. Complete hepatic regeneration after somatic deletion of an albumin-plasminogen activator transgene. Cell 1991;66:245-256.
21. Oinonen T, Lindros KO. Hormonal regulation of the zonated expression of cytochrome P-450 3A in rat liver. Biochem J 1995;309:55-61.
22. Sonnier M, Cresteil T. Delayed ontogenesis of CYP1A2 in the human liver. Eur J Biochem 1998;251:893-898.
23. Sell S. Is there a liver stem cell? Cancer Res 1990;50:3811-3815.
24. Thorgeirsson SS. Hepatic stem cells. Am J Pathol 1993;142:1331-1333.
25. Shafritz DA, Oertel M, Menthena A, Nierhoff D, Dabeva MD. Liver stem cells and prospects for liver reconstitution by transplanted cells. HEPATOLOGY 2006;43(Suppl):89S-98S.
26. Masson NM, Currie IS, Terrace JD, Garden OJ, Parks RW, Ross JA. Hepatic progenitor cells in human fetal liver express the oval cell marker Thy-1. Am J Physiol Gastrointest Liver Physiol 2006;291:G45-G54.
27. Petersen BE, Goff JP, Greenberger JS, Michalopoulos GK. Hepatic oval cells express the hematopoietic stem cell marker Thy-1 in the rat. HEPATOLOGY 1998;27:433-445.
28. Gordon GJ, Coleman WB, Grisham JW. Temporal analysis of hepatocyte differentiation by small hepatocyte-like progenitor cells during liver regeneration in retrorsine-exposed rats. Am J Pathol 2000;157:771-786.
29. Strick-Marchand H, Morosan S, Charneau P, Kremsdorf D, Weiss MC. Bipotential mouse embryonic liver stem cell lines contribute to liver regeneration and differentiate as bile ducts and hepatocytes. Proc Natl Acad Sci U S A 2004;101:8360-8365.
30. Katayama S, Tateno C, Asahara T, Yoshizato K. Size-dependent *in vivo* growth potential of adult rat hepatocytes. Am J Pathol 2001;158:97-105.
31. Mitaka T, Mikami M, Sattler GL, Pitot HC, Mochizuki Y. Small cell colonies appear in the primary culture of adult rat hepatocytes in the presence of nicotinamide and epidermal growth factor. HEPATOLOGY 1992;16:440-447.
32. Asahina K, Shiokawa M, Ueki T, Yamasaki C, Aratani A, Tateno C, et al. Multiplicative mononuclear small hepatocytes in adult rat liver: their isolation as a homogeneous population and localization to periportal zone. Biochem Biophys Res Commun 2006;342:1160-1167.
33. Yoshizato K. Growth potential of adult hepatocytes in mammals: highly replicative small hepatocytes with liver progenitor-like traits. Dev Growth Differ 2007;49:171-184.
34. Gordon GJ, Butz GM, Grisham JW, Coleman WB. Isolation, short-term culture, and transplantation of small hepatocyte-like progenitor cells from retrorsine-exposed rats. Transplantation 2002;73:1236-1243.
35. Brown JJ, Parashar B, Moshage H, Tanaka KE, Engelhardt D, Rabbani E, et al. A long-term hepatitis B viremia model generated by transplanting nontumorigenic immortalized human hepatocytes in Rag-2-deficient mice. HEPATOLOGY 2000;31:173-181.
36. Malhi H, Irani AN, Gagandeep S, Gupta S. Isolation of human progenitor liver epithelial cells with extensive replication capacity and differentiation into mature hepatocytes. J Cell Sci 2002;115:2679-2688.
37. Nowak G, Ericzon BG, Nava S, Jaksch M, Westgren M, Sumitran-Holgersson S. Identification of expandable human hepatic progenitors which differentiate into mature hepatic cells *in vivo*. Gut 2005;54:972-979.

Journal of General Virology (2008), **89**, 2108–2113 DOI 10.1099/vir.0.83658-0

Establishment of an infectious genotype 1b hepatitis C virus clone in human hepatocyte chimeric mice

Takashi Kimura,[1,2] Michio Imamura,[1,2] Nobuhiko Hiraga,[1,2] Tsuyoshi Hatakeyama,[1,2] Daiki Miki,[1,2] Chiemi Noguchi,[1,2] Nami Mori,[1,2] Masataka Tsuge,[1,2] Shoichi Takahashi,[1,2] Yoshifumi Fujimoto,[1,2] Eiji Iwao,[3] Hidenori Ochi,[2,4] Hiromi Abe,[1,2,4] Toshiro Maekawa,[4] Keiko Arataki,[5] Chise Tateno,[2,6] Katsutoshi Yoshizato,[2,6] Takaji Wakita,[7] Toru Okamoto,[8] Yoshiharu Matsuura[8] and Kazuaki Chayama[1,2,4]

Correspondence
Kazuaki Chayama
chayama@hiroshima-u.ac.jp

[1]Department of Medicine and Molecular Science, Division of Frontier Medical Science, Programs for Biomedical Research, Graduate School of Biomedical Sciences, Hiroshima University, Hiroshima, Japan

[2]Liver Research Project Center, Hiroshima University, Hiroshima, Japan

[3]Research Division, Mitsubishi Tanabe Pharma Corporation, Osaka, Japan

[4]Laboratory for Liver Disease, SNP Research Center, Institute of Physical and Chemical Research (RIKEN), Yokohama, Japan

[5]Hirosimakinen-Hospital, Internal Medicine, Hiroshima, Japan

[6]Developmental Biology Laboratory, Department of Biological Science, Graduate School of Science, Hiroshima University, Higashihiroshima, Japan

[7]Department of Virology II, National Institute of Infectious Diseases, Shinjuku-ku, Japan

[8]Department of Molecular Virology, Research Institute for Microbial Diseases, Osaka University, Osaka, Japan

The establishment of clonal infection of hepatitis C virus (HCV) in a small-animal model is important for the analysis of HCV virology. A previous study developed models of molecularly cloned genotype 1a and 2a HCV infection using human hepatocyte-transplanted chimeric mice. This study developed a new model of molecularly cloned genotype 1b HCV infection. A full-length genotype 1b HCV genome, HCV-KT9, was cloned from a serum sample from a patient with severe acute hepatitis. The chimeric mice were inoculated intrahepatically with *in vitro*-transcribed HCV-KT9 RNA. Inoculated mice developed viraemia at 2 weeks post-infection, and this persisted for more than 6 weeks. Passage experiments indicated that the sera of these mice contained infectious HCV. Interestingly, a similar clone, HCV-KT1, in which the poly(U/UC) tract was 29 nt shorter than in HCV-KT9, showed poorer *in vivo* infectivity and replication ability. An *in vitro* study showed that no virus was produced in the culture medium from HCV-KT9-transfected cells. In conclusion, this study developed a genetically engineered genotype 1b HCV-infected mouse. This mouse model will be useful for the study of HCV virology, particularly the mechanism underlying the variable resistance of HCV genotypes to interferon therapy.

Received 13 December 2007
Accepted 14 May 2008

INTRODUCTION

Hepatitis C virus (HCV), a positive-sense, single-stranded RNA virus, infects and replicates efficiently only in the hepatocytes of humans and chimpanzees. There are many genotypes of HCV distributed worldwide (Simmonds *et al.*, 1993); among them genotype 1b is the major genotype in Asia, including Japan, and is known to be one of the most resistant genotypes to interferon (IFN) therapy (Fried *et al.*, 2002). Until recently, studies of HCV replication have long been hampered by the lack of a virus culture system. The development of HCV replicon systems has allowed the

The GenBank/EMBL/DDBJ accession numbers for the sequences of HCV-KT9 and HCV-KT1 determined in this work are AB435162 and AB426117, respectively.

study of the mechanisms of replication of HCV (Lohmann *et al.*, 1999). However, these replicons lack structural proteins, do not replicate efficiently without adaptive mutations and do not produce infectious virions. Recently, it was reported that the genotype 2a full-length JFH-1 genome replicated efficiently in Huh7 cells without adaptive mutations and produced virions that were infectious for both naïve cells and chimpanzees, as well as for a human hepatocyte-transplanted chimeric mouse (Wakita *et al.*, 2005; Zhong *et al.*, 2005; Lindenbach *et al.*, 2006). To date, five full-length genotype 1b clones, HCV-N (Beard *et al.*, 1999), Con-1 (Bukh *et al.*, 2002), HCV-J4 (Okamoto *et al.*, 1992), HCV-CG1b (Thomson *et al.*, 2001) and HCV-BK (Takamizawa *et al.*, 1991), have been demonstrated to be infectious by intrahepatic inoculation of transcribed HCV RNA into the liver of chimpanzees. Among these, only the HCV-CG1b genome is reported to produce HCV particles when transfected into Huh7 cells (Heller *et al.*, 2005).

Although the chimpanzee is a useful animal model for the study of HCV infection, there are ethical restrictions on the use of this animal. Instead, Mercer *et al.* (2001) developed a useful small-animal model for the study of HCV infection using chimeric urokinase-type plasminogen activator (uPA)/severe combined immunodeficiency (SCID) mice (which are immunodeficient and undergo liver failure) with engrafted human hepatocytes. This HCV-infected mouse model is reported to be useful for evaluating anti-HCV drugs such as IFN-α and anti-NS3 protease (Kneteman *et al.*, 2006). We have previously described methods to improve the replacement levels of human hepatocytes in this mouse model (Tateno *et al.*, 2004) and we have developed a reverse genetics system for hepatitis B virus (Tsuge *et al.*, 2005) and HCV (Hiraga *et al.*, 2007). In the present study, we report the establishment of an infectious genotype 1b HCV clone that infects and replicates efficiently in human hepatocyte chimeric mice.

METHODS

Cloning of infectious genotype 1b HCV isolate. Serum samples were obtained from a 43-year-old physician who developed severe acute hepatitis after needle stick exposure from a patient with chronic hepatitis C. On admission, the serum total bilirubin concentration was 10.0 mg dl^{-1} and the prothrombin time was 40 %. The patient tested positive for HCV antibodies by a third-generation radioimmunoassay (Ortho-Clinical Diagnostics) and for HCV RNA by RT-PCR. Serum HCV RNA was quantified using an Amplicor Monitor HCV test (Roche Diagnostics). The HCV RNA titre was 2.5×10^6 copies ml^{-1} on admission and then decreased gradually. Fig. 1 shows the serial changes in alanine aminotransferase (ALT) as a measure of liver function and HCV RNA levels in this patient. Serum samples obtained in the early phase of infection were used for cloning the full-length genome.

RNA extraction, cDNA synthesis, plasmid construction and RNA transcription. Total RNA was extracted from 100 µl serum samples using SepaGene RV-R (Sanko Junyaku) and reverse transcribed with random hexamers and ReverTra Ace reverse transcriptase (Toyobo) according to the manufacturer's instructions. PCR primers were designed based on the sequence of HCV-Con1 (GenBank accession no. AJ238799; Bukh *et al.*, 2002). Five overlapping cDNA segments (nt 1–2292, 2269–6715, 6696–9094, 7564–9404 and 9361–9605; nucleotide numbers are those of HCV-Con1) were amplified by PCR with TaKaRa LA *Taq* polymerase (Takara Biochemicals) using the above cDNA. Amplified products were separated by agarose gel electrophoresis. Nucleotide sequences were determined using a Big Dye Terminator Mix Cycle Sequencing kit (Applied Biosystems Japan) with an automated DNA sequencer (model 310; PE Biosystems). We corrected the nucleotide sequences of the obtained clones by site-directed mutagenesis and made them identical to the nucleotide sequences obtained by direct sequencing. Naturally occurring restriction enzyme cutting sites were utilized to clone each segment. We utilized the vector pBR322 and created a multiple-cloning site under the control of the T7 promoter by ligating a linker at restriction enzyme cutting sites as they appeared in order from 5′ to 3′ in the HCV sequences (Fig. 2a). Each segment of HCV was cloned into this vector to generate the full-length clones. The HCV-KT9 clone was established using the 3′-terminal fragment with the longest poly(U/UC) tract length (115 nt), which should have a high replication ability (Friebe & Bartenschlager, 2002; Yi & Lemon, 2003; You & Rice, 2008). A clone with a shorter poly(U/UC) tract length (86 nt), HCV-KT1, was also generated. A polymerase-deficient mutant with an amino acid substitution in the GDD motif (GDD→GND; HCV-KT9-GND) was generated using a Quick Change Site-Directed Mutagenesis kit (Stratagene). After digesting the plasmid with *Xba*I (New England BioLabs) at the 3′ end of the HCV cDNA, HCV RNA was transcribed using T7 RNA polymerase (MEGAscript; Ambion) at 37 °C for 3 h in a 100 µl reaction mixture, according to the manufacturer's instructions. The RNA was analysed using denaturing agarose gel electrophoresis and kept at −80 °C until use.

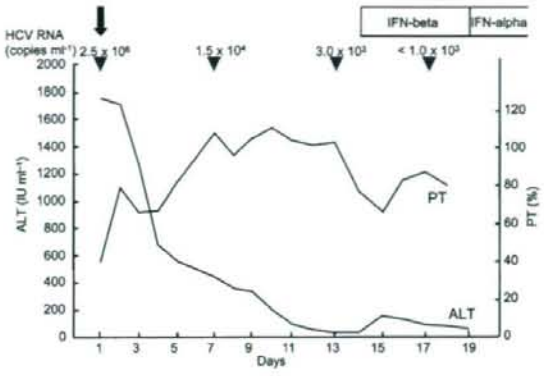

Fig. 1. Clinical course of a patient with severe acute hepatitis C. Alanine aminotransferase (ALT) and prothrombin time (PT) are shown from the day of admission (day 1). The patient was treated daily with 10^6 U IFN-β intravenously for 5 days, followed by 10^6 U IFN-α intramuscularly three times a week for 6 months. HCV RNA was measured on days 1, 7, 13 and 17 (arrowheads). A serum sample was taken on day 1 (arrow) and used to clone the full-length HCV genome.

Construction of a phylogenetic tree. A phylogenetic tree was constructed based on the entire nucleotide sequences of 26 full-length genotype 1b clones plus HCV-KT9. The total number of synonymous and non-synonymous substitutions among the nucleotide sequences was estimated using the method of Gojobori *et al.* (1982) and a phylogenetic tree was constructed by the neighbour-joining method (Saitou & Nei, 1987).

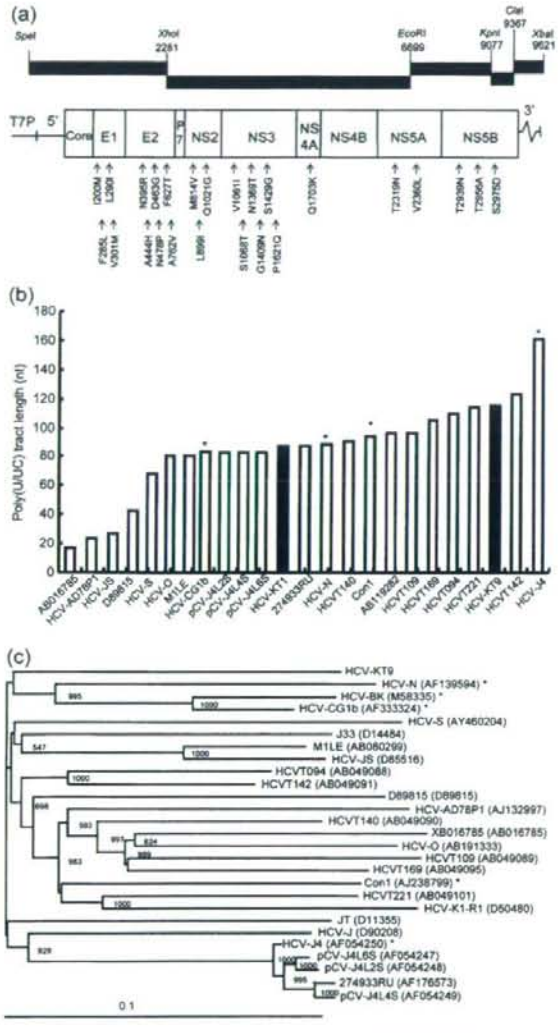

Fig. 2. (a) Schematic diagram of the organization of the cDNA clone HCV-TK9. The T7 RNA promoter (T7P) is located immediately upstream of the HCV genome. Restriction enzyme sites that were used to create clone HCV-KT9 are labelled according to their nucleotide position within the HCV sequence. Amino acid sequences unique to HCV-KT9 compared with 26 other HCV genotype 1b isolates are indicated at the bottom of the figure, with the position of the repaired amino acid residues noted within the polyprotein. (b) Length of the poly(U/UC) tracts of HCV-KT1, HCV-KT9 and 22 other HCV genotype 1b clones reported previously. Asterisks indicate clones confirmed to be infectious by experiments using chimpanzees. (c) Phylogenetic tree constructed with HCV-KT9 and 26 genotype 1b HCV whole-genome sequences. Bar, number of nucleotide substitutions per site. Asterisks indicate clones confirmed to be infectious in experiments using chimpanzees.

Intrahepatic injection experiments in human hepatocyte chimeric mice. We used methods described previously (Tateno *et al.*, 2004) to generate uPA$^{+/+}$/SCID$^{+/+}$ mice and transplant human hepatocytes. All mice used in this study were transplanted with frozen human hepatocytes obtained from the same donor. Mouse serum concentrations of human serum albumin (HSA) correlate with the repopulation index and were measured as described previously (Tateno *et al.*, 2004). Intrahepatic injection of RNA, extraction of serum samples and euthanasia were performed under ether anaesthesia. Briefly, 500 µl RNA solution containing 30 µg transcribed HCV RNA was injected into the liver of anaesthetized chimeric mice through a small abdominal incision. RNA extraction from mouse serum samples, quantification of HCV RNA and nested PCR were performed as described previously (Hiraga *et al.*, 2007). All animal protocols described in this study were performed in accordance with the guidelines of the local committee for animal experiments and under the approval of the Ethics Review Committee for Animal Experimentation of the Graduate School of Biomedical Sciences, Hiroshima University.

Cell culture, RNA transfection and measurement of HCV core antigen. The human hepatoma cell line Huh7 was maintained in Dulbecco's modified Eagle's medium (Sigma) containing 10% fetal calf serum. RNA transfection and measurement of HCV core antigen in the culture medium were performed as described previously (Wakita *et al.*, 2005).

Statistical analysis. The infectious ratio of chimeric mice was compared and the differences assessed using a χ^2 test. Differences in HCV RNA replication ability *in vitro* were analysed statistically by one-way analysis of variance followed by Scheffe's test. A P value of less than 0.05 was considered statistically significant.

RESULTS

Characteristics of genotype 1b clones HCV-KT9 and HCV-KT1

The entire genome of HCV cDNA was assembled from five DNA fragments (Fig. 2a). We obtained 24 3′-extremity clones with different poly(U/UC) tract lengths. We selected the clone with the longest (U/UC) tract because a previous study indicated that the length of poly(U/UC) tract correlates with HCV replication in an HCV replicon system (Friebe & Bartenschlager, 2002; Yi & Lemon, 2003; You & Rice, 2008). The length of the poly(U/UC) tract in the longest 3′ clone was 115 nt. The entire genome length of the HCV-KT9 clone using this longest 3′ clone was 9621 nt. We also generated the clone HCV-KT1 with a shorter (86 nt) poly (U/UC) tract to compare the replication abilities of these clones. The lengths of the poly(U/UC) tracts of 22 clones deposited in GenBank are shown in Fig. 2(b). All infectious clones had a poly(U/UC) tract longer than 80 nt. Fig. 2(c) shows a phylogenetic tree constructed using the nucleotide sequences of the 26 full-length genotype 1b clones published to date. Interestingly, the sequence of HCV-KT9 was closest to that of HCV-CG1b (GenBank accession no. AF333324), which has been reported to be infectious, and formed a cluster with two other infectious clones, HCV-N (Beard *et al.*, 1999) and HCV-BK (Takamizawa *et al.*, 1991). We compared the amino acid

sequences of HCV-KT9 with an alignment of the sequences of the 26 other genotype 1b strains. All HCV full-length clones reported from Japan were included in these 26 strains. Based on these comparisons, we identified 25 aa unique to HCV-KT9 (Fig. 2a). We found that the amino acid sequence of the IFN sensitivity-determining region in the NS5A region, which has been suggested to mediate IFN resistance via interaction with the cellular protein kinase R (Enomoto *et al.*, 1996; Gale *et al.*, 1997), was that of the wild-type.

Intrahepatic injection of HCV-KT1 and HCV-KT9 RNAs into human hepatocyte chimeric mice

In the next experiments, 30 μg *in vitro*-transcribed RNA of HCV-KT1, HCV-KT9 or HCV-KT9-GND was injected into the livers of chimeric mice. Eight of 10 (80 %) HCV-KT9-injected mice developed measurable viraemia at 2 weeks post-inoculation (Table 1 and Fig. 3), with the HCV RNA titre reaching 1.1×10^6 to 8.8×10^6 copies ml^{-1} at 6 weeks post-inoculation (Fig. 3). To check for the presence of infectious HCV in the serum of HCV-KT9-infected mice, each of five naïve mice was injected with 10 μl serum sample (containing 3.5×10^5 copies of HCV) obtained from an HCV-KT9-infected mouse 6 weeks after inoculation. All five naïve mice became positive for HCV RNA, as confirmed by nested PCR, at 2 weeks post-inoculation and two mice developed persistent viraemia (Fig. 4). These results indicated that the serum of HCV-KT9-injected mice contained infectious HCV. In contrast to HCV-KT9, none of the three mice injected with HCV-KT9-GND RNA developed viraemia (Table 1). These results indicated that HCV-KT9 replicates efficiently in mice livers and produces infectious virus continuously. On the other hand, only one out of seven HCV-KT1-injected mice (14 %) developed measurable viraemia (Table 1 and Fig. 3). The level of viraemia was low in this HCV-KT1-infected mouse, HCV RNA was negative by nested PCR at 2 weeks after inoculation and the titre was only 2.2×10^4 copies ml^{-1} at 4 weeks post-inoculation (Fig. 3). These results confirmed the importance of the poly(U/UC) tract length in experimentally induced viraemia.

The nucleotide and amino acid sequences of the viral genome isolated from an HCV-KT9-injected mouse (Fig. 3) at 6 weeks after RNA injection were identical to the injected HCV-KT9 (data not shown). We tried to reclone the poly(U/UC) tract in the HCV-KT1-infected mouse, but it was impossible to reamplify the HCV cDNA using the remaining small amount of serum.

Table 1. Correlation between length of the poly(U/UC) tract and HCV infection

Clone	Length of poly(U/UC) tract	Number of mice			Infection ratio
		Infected	Not infected	Total	
HCV-KT1	86	1	6	7	14 %
HCV-KT9	115	8	2	10	80 %*
HCV-KT9-GND	115	0	3	3	0 %

*P=0.015, compared with HCV-KT1.

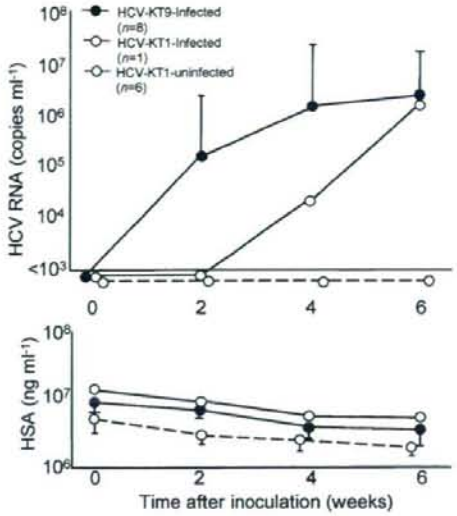

Fig. 3. Changes in HCV RNA levels and HSA concentrations in the sera of mice infected with clonal HCV. Mice were inoculated intrahepatically with 30 μg *in vitro*-transcribed HCV RNA. Eight of the ten HCV-KT9-infected mice (80 %), one of the seven HCV-KT1-infected mice (14 %) and none of the three HCV-KT9-GND-infected mice became positive for HCV RNA. The results for six HCV-KT1-uninfected mice are also shown. Mice serum samples were obtained every 2 weeks post-infection for analysis of HCV RNA titres. Data are shown as mean ± SD.

Analysis of virus production from HCV-KT9-transfected cells

Next, we evaluated the ability of the HCV-KT9 clone to replicate in transfected Huh7 cells. In these experiments, we used JFH-1 RNA, which is known to replicate efficiently in cell cultures, as control (Wakita *et al.*, 2005). Core protein was secreted efficiently from JFH-1 RNA-transfected Huh7 cells. In contrast, we did not observe any measurable levels of core protein in the supernatant of HCV-KT9-transfected cells (Fig. 5), suggesting a minimal replication ability of HCV-KT9 to produce and release virus into the supernatant.

DISCUSSION

In this study, we described the establishment of a genotype 1b clone, HCV-KT9, that replicated efficiently following injection of the transcribed RNA into chimeric mouse liver.

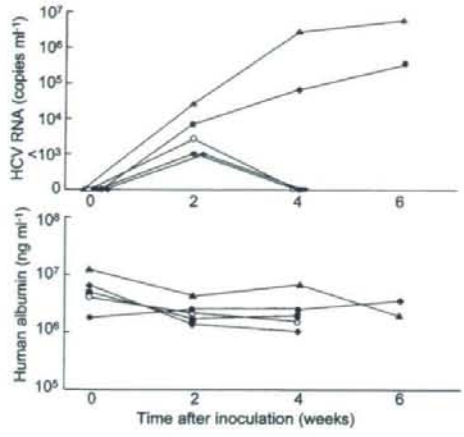

Fig. 4. Passage experiments of HCV in naïve chimeric mice. Five naïve chimeric mice were inoculated intravenously with 10 µl serum sample (containing 3.5×10^5 copies HCV) obtained from an HCV-KT9-infected mouse at week 6 post-inoculation. Serum samples were obtained at the indicated time intervals for the measurement of HCV RNA levels and HSA concentrations. Data represent the changes in five individual mice.

The key factor that determines the infectivity of HCV clones has not yet been established. We previously established a clone from HCV that replicated in a chimeric mouse after injection of serum from a chronically HCV-infected patient. However, we did not observe viraemia after intrahepatic injection of the transcribed RNA from this clone (unpublished results). In contrast, injection of HCV-KT9 RNA in the present study resulted in viraemia in eight out of ten mice (80 %). The fact that the nucleotide and amino acid sequences of the virus recovered from the infected mice were identical to those of the HCV-KT9 clone indicated that no adaptive mutation was necessary for this clone to replicate in the chimeric mouse.

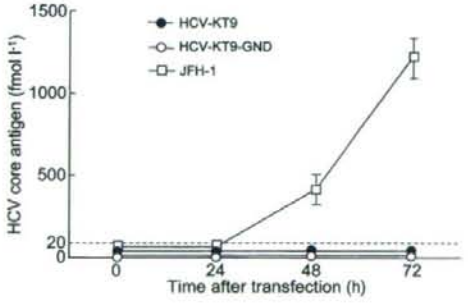

Fig. 5. Time-course studies of HCV core protein secretion into the culture medium of HCV RNA-transfected cells. Huh7 cells were transfected with 10 µg HCV-KT9, HCV-KT9-GND or JFH-1 RNA. HCV core antigen in the culture medium was measured at 24, 48 and 72 h after transfection. Data are shown as mean ± SD of HCV core protein levels obtained from three independent transfection experiments.

Interestingly, the clone was obtained from a patient with severe acute hepatitis. This is similar to JFH-1, an HCV clone with a strong replication ability in cultured cell lines, chimpanzees and chimeric mice, which was cloned from serum samples of a patient who developed acute fulminant hepatitis with a high virus titre (Wakita *et al.*, 2005). A virus that replicates in the early stage of infection may have strong replication ability, which may be lost in the chronic phase of infection.

A key amino acid substitution may be present in one (or some) of the amino acids unique to this clone (Fig. 2a). We also showed that clone HCV-KT1, which differs from HCV-KT9 only in the length of the poly(U/UC) tract, had a poorer replication ability in mice (Table 1 and Fig. 3). However, there is a possibility that a shorter poly(U/UC) tract only slows down the rate of infection, as the HCV RNA titre in the HCV-KT1-infected mouse at 6 weeks after inoculation was similar to that in HCV-KT9-infected mice (Fig. 3). It has been reported that the length and composition of the poly(U/UC) tract is important for the replication of HCV replicons (Friebe & Bartenschlager, 2002; Yi & Lemon, 2003; You & Rice, 2008). However, no replication advantage of a poly(U/UC) tract longer than 86 bp was revealed in this study. This may be due to differences *in vitro* and *in vivo*, where the innate immune response against the virus may be more robust than in cell culture.

As shown in the present study, reverse genetics of HCV has become available for studies of HCV replication. The important factors for virus replication suggested above can be analysed further using this system.

We also examined the response of HCV-KT9-infected mice to IFN treatment. Three HCV-KT9-infected mice were treated with daily intramuscular injections of 1000 IU IFN-α (g body weight)$^{-1}$ for 2 weeks. This regimen resulted in a reduction in HCV RNA levels of only 1.0 log copies ml^{-1} (data not shown). These results are consistent with our previous study, which showed a similar low-level reduction in HCV RNA in mice infected with a genotype 1a clone, and differ from our previous results in mice infected with HCV genotype 2a, which became negative for HCV RNA following daily treatment with 1000 IU IFN-α (g body weight)$^{-1}$ for 2 weeks (Hiraga *et al.*, 2007). These results are in agreement with our clinical experience that genotype 1 is more resistant to IFN therapy than genotype 2. As shown in the present study and previously (Hiraga *et al.*, 2007), reverse genetics of HCV with three genotypes, 1a, 1b and 2a, is now available. By recombination of these clones or the establishment of mutants with nucleotide and amino acid sequences similar to each other, it may be possible to clarify the mechanism underlying the variability in susceptibility of HCV genotypes to IFN.